Scientific Reports

https://doi.org/10.1038/s41598-026-39106-1

Article in Press

EEG-based predictors of motor recovery during immersive VR-BCI rehabilitation

Received: 11 December 2025

Accepted: 3 February 2026

Published online: 09 February 2026

Cite this article as: Valente M., Branco D., Bermúdez i Badia S. *et al.* EEG-based predictors of motor recovery during immersive VR-BCI rehabilitation. *Sci Rep* (2026). https://doi.org/10.1038/s41598-026-39106-1

Madalena Valente, Diogo Branco, Sergi Bermúdez i Badia, Jean-Claude Fernandes, Patrícia Figueiredo & Athanasios Vourvopoulos

Baseline Sensorimotor EEG and Its Longitudinal Change as Predictors of Motor Recovery During VR-BCI Rehabilitation: A Randomized Pilot Trial

Madalena Valente [1], Diogo Branco [2,3], Sergi Bermúdez i Badia [2,3], Jean-Claude Fernandes [1,4], Patrícia Figueiredo [1], Athanasios Vourvopoulos [1,*]

[1]Institute for Systems and Robotics - Lisboa, Bioengineering Department, Instituto Superior Técnico, Universidade de Lisboa, Lisboa, Portugal
[2]Faculty of Exact Sciences and Engineering & NOVA LINCS, University of Madeira, Funchal, Portugal
[3]ARDITI - Agência Regional para o Desenvolvimento da Investigação, Tecnologia e Inovação, Funchal, Portugal
[4]Physical Medicine and Rehabilitation Service, Central Hospital of Funchal, Funchal, Portugal

E-mail: *athanasios.vourvopoulos@tecnico.ulisboa.pt

Abstract. Motor impairment following stroke frequently leads to long-term disability, limiting independence and quality of life. Brain–Computer Interface (BCI) systems integrating motor imagery (MI) with virtual reality (VR) offer promising avenues for enhancing neuroplasticity and engagement through immersive, real-time, and proprioceptive feedback. Yet, identifying reliable electroencephalography (EEG)-based biomarkers that reflect or predict recovery remains challenging. This study investigated the relationship between event-related desynchronization (ERD) dynamics during MI–VR training and motor recovery in individuals with chronic stroke. Fourteen participants with stroke (9 experimental, 5 control) completed a 4-week VR–BCI intervention and were compared with a non-stroke reference cohort (N = 35). Linear mixed-effects models assessed ERD modulation across sessions and groups, and a two-stage regression evaluated the predictive value of ERD features for Fugl–Meyer Assessment (FMA) gains. Results showed no significant ERD change across sessions, but stroke participants exhibited significantly reduced ERD compared to controls. Baseline ERD amplitude predicted motor improvement, whereas ERD progression did not. Ipsilateral ERD showed a compensatory trend in ischemic stroke. These findings indicate that baseline ERD may serve as a stronger prognostic biomarker than short-term ERD dynamics, supporting the development of personalized VR–BCI rehabilitation strategies for chronic stroke recovery.

Keywords: Brain-Computer Interfaces, Motor Imagery, Event-Related Desynchronization, Stroke Rehabilitation, Virtual Reality

1. Introduction

Stroke continuous to be a leading cause of disability worldwide, often resulting in motor impairments that significantly affect patients' quality of life [1]. Among these impairments, hemiparesis affecting the upper limb is particularly common [2], with many survivors experiencing chronic limitations despite receiving conventional rehabilitation therapies [3].

Current stroke upper–limb rehabilitation combines traditional neurofacilitation methods, which remain widely used in clinical practice, with more contemporary task-specific approaches that emphasize movement re-education and functional training. These rehabilitation strategies are increasingly complemented by technology-based interventions such as functional electrical stimulation (FES), robotic-assisted therapy, and virtual reality (VR) [4, 5, 6].

Evidence supports the use of Brain–Computer Interfaces (BCI) for post-stroke rehabilitation, especially for upper limb motor recovery, with numerous meta-analyses reporting moderate to large beneficial effect sizes [7, 8, 9, 10]. One of the earliest randomized controlled trials (RCT) providing direct evidence of BCI efficacy, showing significantly greater improvements in upper-limb motor function compared to motor imagery (MI) practice alone in subacute stroke patients [11]. Specifically, BCI training significantly improves clinical measures like the Fugl–Meyer Assessment–Upper Extremity (FMA-UE; MD = 3.69) and the Action Research Arm Test (ARAT) [12, 13], often demonstrating superior results compared to conventional rehabilitation [14, 15, 12]. The interventions are widely considered safe for clinical use [16, 9, 13].

The efficacy relies on the BCI's ability to promote neuroplasticity by creating a closed-loop system linking the patient's neural intent (e.g., motor imagery) with real-time sensory/motor feedback, which reinforces damaged motor circuits via Hebbian learning [17, 18, 12]. Specifically, MI and motor observation (MO) are commonly employed in electroencephalography (EEG)–based BCI protocols, as both processes are associated with the activation of the sensorimotor cortex and the mirror neuron system (MNS) [19]. These activities induce event-related desynchronization (ERD) in the Alpha (8-12 Hz) and Beta (12-30 Hz) bands, which are neural markers linked to motor planning, execution, and motor recovery [20].

Specifically, enhanced ERD in stroke rehabilitation is consistently linked to improved BCI control and motor recovery, with stronger ipsilesional ERD indicating better neuroplastic adaptation [21, 22, 23, 24, 25]. Cortical lesions typically show greater reductions in ipsilesional alpha and beta ERD, while subcortical lesions display more variable, often bilateral patterns [23]. However, variability in study methodologies hampers synthesis and comparability [23]. Further, greater ERD lateralization toward the ipsilesional hemisphere generally predicts better motor outcomes [26, 21, 22, 27], and correlations between ERD metrics—such as the Laterality Coefficient—support its value as a predictive biomarker [27, 28]. Nonetheless, contralesional or bilateral ERD patterns in severe cases challenge the generalisation of ipsilesional dominance [29].

Baseline Sensorimotor EEG and Its Longitudinal Change.

EEG–based BCIs are advantageous due to their non-invasive nature, portability, and cost-effectiveness. Recent reviews underscore the need for prognostic neurophysiological markers that can inform personalized rehabilitation strategies and improve patient stratification [30, 31]. However, the effectiveness of MI-BCI training varies widely across individuals, with factors such as lesion location, cognitive status, and MI ability contributing to this variability [32, 33, 34, 35]. Moreover, BCI performance often suffers from inadequate feedback or unstable EEG signals [36], thereby hindering effective learning [37] and reinforcing the value of co-adaptive or mutual learning paradigms [38]. Recent research has explored deep learning algorithms to adapt BCIs to individual neural signatures, though traditional machine learning methods often yield comparable results [39].

Integrating VR into BCI training is a promising strategy to enhance motor rehabilitation. VR provides immersive, first-person experiences that can induce a sense of embodiment, allowing patients to visualize and experience virtual limb movements even without physical execution. Prior findings have been shown increased embodiment, higher sensorimotor brain activity, and improved accuracy of task execution in immersive VR environments compared to conventional screen feedback. Pilot studies indicated enhanced motivation, focus, and motor outcomes for stroke and healthy subjects [40, 41, 42, 43, 44]. Further, employing a virtual therapist with augmented feedback within VR, have showed showed promising results in neuro–motor recovery [45]. VR environments also offer safe, engaging, and motivating settings for rehabilitation, with gamified tasks that have been shown to enhance engagement and adherence to therapy [6].

Despite growing evidence supporting the use of VR–BCI systems for stroke rehabilitation, the relationship between brain activity modulation and clinical outcomes remains insufficiently understood. Specifically, the long-term effects of VR–BCI training on motor function and its correlation with neurophysiological changes, such as Alpha and Beta ERD patterns, require further investigation. This need is driven by high inter- and intra-subject variability in neural responses [46], which can arise from differences in stroke severity, location, and levels of engagement. Additionally, the variability in training protocols further complicates our understanding of how neurophysiological adaptation supports motor learning and recovery [36].

While the clinical efficacy of VR-BCI system for post-stroke motor rehabilitation has been demonstrated in previous studies, this study aims to bridge existing knowledge gaps by identifying EEG-based neural features that may predict individual responsiveness to therapy. Building on previous work, this study ensures consistency of the experimental paradigm, feedback design, and analysis pipeline, addressing the persistent lack of standardization across BCI studies. By examining the interaction between motor recovery and neural activity, this work seeks to advance the development of more effective and personalized BCI–based neurorehabilitation strategies for individuals with chronic and severe motor impairments.

Baseline Sensorimotor EEG and Its Longitudinal Change.

2. Methods

2.1. Participants

Fourteen individuals with stroke were recruited between August 2019 and December 2023 and randomly allocated in two groups. Recruitment was disrupted by COVID-19–related hospital restrictions. Ultimately, nine were allocated to the experimental group (four female), and five (one female) served as a control group (Table 1). The final sample was unbalanced due to participant dropouts over the course of the study. Participants provided their written informed consent in accordance with the Declaration of Helsinki. This study was approved by Scientific and Ethic Committees of the Central Hospital of Funchal, Portugal - approval: 21/2019 with a clinical trial registration number: NCT04376138. No interim analyses were planned; however, all study sessions were conducted at the hospital, allowing prompt response in case of medical need and enabling standardized stopping guidelines if necessary. The control group received standard care. All participants continued their usual therapy; no additional rehabilitation was provided. Harms were defined as any adverse events or unintended effects related to study procedures (e.g., discomfort, dizziness, anxiety, technical intolerance) and were monitored non-systematically through self-report and investigator observation. No adverse events were reported in either group. Further, data from 35 individuals without stroke were used as a reference cohort. This diverse dataset provides a baseline for comparing neurophysiological responses observed in individuals with stroke. These participants followed the same VR-BCI protocol and experimental setup as the stroke group, ensuring methodological consistency across cohorts.

Table 1: Demographic and Clinical Profile of Participants with Stroke. Participants are divided into two groups: experimental and control. MPS refers to Months Post-Stroke. FMA refers to the Fugl-Meyer Assessment for the upper limb (maximum value = 66). ΔFMA is the change between pre- and post-FMA scores, with * indicating minimal clinically important difference (MCID). MoCA refers to the Montreal Cognitive Assessment (maximum score = 30). ΔMoCA is the difference between pre- and post-MoCA scores. Follow-up assessment was performed a month after they finished the intervention.

Participant ID	Group	Gender	Age (years)	Stroke Type	Lesion Type	MPS (months)	Affected Side	FMA				MoCA			
								Pre	Post	Follow-up	Δ	Pre	Post	Follow-up	Δ
P01	Experimental	F	48	Hemorrhagic	Mixed	11.3	Right	22	19	19	-3	25	21	25	-4
P02	Experimental	F	63	Ischemic	Subcortical	181.5	Left	40	47	40	7*	28	22	26	-6
P05	Experimental	M	61	Ischemic	Mixed	79.1	Left	58	58	58	0	26	26	30	0
P08	Experimental	M	58	Ischemic	Mixed	11.3	Left	13	21	20	8*	19	23	24	4
P03	Experimental	F	64	Hemorrhagic	Mixed	17	Left	42	58	59	16*	10	12	19	2
P21	Experimental	M	59	Ischemic	Brainstem	9	Right	62	62	62	0	22	24	26	2
P24	Experimental	M	65	Hemorrhagic	Mixed	8	Right	50	52	57	2	15	15	15	0
P40	Experimental	F	54	Ischemic	-	21	Left	50	52	-	2	-	-	-	-
C01	Control	M	56	Ischemic	Mixed	64.5	Left	15	21	20	6*	23	26	25	3
C02	Control	M	54	Hemorrhagic	Disperse small vessel disease	5.4	Right	43	51	53	8*	22	25	20	3
C03	Control	F	54	Ischemic	Mixed	4.9	Left	12	16	21	4*	19	18	22	-1
C04	Control	M	51	Ischemic	Subcortical	26.2	Right	29	43	48	14*	27	27	30	0
C05	Control	M	58	Ischemic	Mixed	168.1	Right	39	36	-	-3	13	16	-	3

Baseline Sensorimotor EEG and Its Longitudinal Change.

2.1.1. Participants with Stroke: Individuals with stroke (N = 14) in the chronic phase (two enrolled at 4.9 and 5.4 months but started > 6 months post-stroke) were recruited at the Central Hospital of Funchal. Mean age was 58 years (SD = 6), 65% male and 35% female, with 4 participants presenting with hemorrhagic stroke and 10 with ischemic stroke (Table 1). The study was originally registered with an expected sample size of 20 participants based on practical considerations rather than a formal power calculation; however, achieving this target proved challenging due to strict eligibility criteria, resulting in an unbalanced final sample (9 experimental, 5 control) following participant dropouts (Figure 1(a)).

The inclusion criteria for participation required upper limb paresis, defined by FME-UE score ≤ 47, with lesion characteristics confirmed via neuroimaging (magnetic resonance imaging or an equivalent modality). Additionally, participants must have experienced a first stroke episode with no documented lasting effects from previous events, possess sufficient cognitive capacity to execute the required tasks. have a minimum of 2 years of formal education. The minimum education requirement reflects local clinical standards for literacy and task comprehension rather than academic attainment. While the clinical trial registration specified an age range of 18 to 80 years, the study protocol included all eligible participants aged ≥ 18 years.

Exclusion criteria included a history of cognitive impairment prior to the stroke and severe aphasia, perceptual, or cognitive deficits that would interfere with task execution or communication. Clinical thresholds for exclusion were set for hemispatial neglect, defined as a score > 6 on the Bells Test, and clinically significant depression, defined as a Beck Depression Inventory (BDI) score > 28 (Portuguese version by Vaz Serra & Pio Abreu, 1973)). Notably, the BDI was utilized as a cross-sectional screening tool at baseline in place of the registered Geriatric Depression Scale (GDS) [47] to better suit the adult population's profile. Participants were also excluded if they presented with other neurological, neuromuscular, or orthopedic conditions affecting motor capacity, severe visual impairment, claustrophobia, or the presence of ferromagnetic material in the body. While muscle tone was systematically assessed using the Modified Ashworth Scale (MAS), spasticity was not a formal exclusion criterion; baseline motor function was evaluated using the FME-UE.

One participant (P39) completed the full intervention and is presented in this study for reference; however, as he did not meet the stroke chronicity criteria (< 6 months), his data were excluded from this analysis.

2.1.2. Participants without Stroke: Participants without stroke (N = 35) were individuals with no history of neurological or other clinically significant medical conditions. The data were obtained from our previous laboratory studies [48, 49, 50], where the experimental setup and protocol were identical to those used for the stroke group (Figure 1(b)). The first group from [50] included 19 participants (mean age = 24.79 years, SD = 3.54), with 13 males and 6 females. Similarly, [48] included 11 participants (mean age = 27.29 years, SD = 4.31), consisting of 8 males and 3

females. Further, [49] included 5 participants (mean age = 51 years, SD = 5.5), 4 of whom were female. Finally, the non-stroke cohort was not age-matched to the stroke cohort. However, in an independent study using the same NeuRow VR-BCI protocol, no significant association between age and MI-BCI performance and no differences between age groups were observed, suggesting minimal age effects within the 20–50 year range typical of our non-stroke datasets [48].

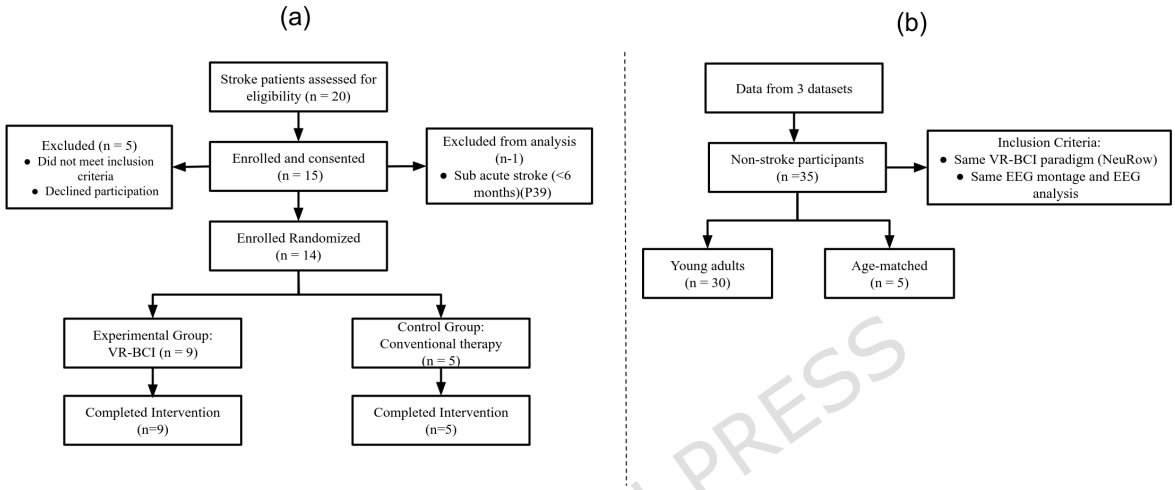

Figure 1: Study flowchart. (a) Flow diagram of participant recruitment, allocation, exclusions, and inclusion in analyses for the prospective stroke cohort. Fifteen individuals with stroke were enrolled; one participant was excluded from analysis for not meeting chronicity criteria ($<$ 6 months post-stroke). Fourteen participants were randomized to either a VR–BCI intervention group or a conventional therapy control group and were included in the final analyses. (b) Flow diagram of the non-stroke reference cohort, pooled from three previously completed studies using the same VR–BCI paradigm and EEG protocol. This cohort (N = 35) was included exclusively for neurophysiological (ERD) reference and was not used for clinical inference.

2.2. Clinical Outcome Measures

The primary clinical outcome measures included the FMA-UE and the Montreal Cognitive Assessment (MoCA). Participants with stroke were assessed pre- and post-intervention, with most undergoing an additional follow-up assessment one month after completing the experimental protocol. Cognitive capacity was not operationalized using a fixed MoCA cut-off, instead, eligibility was determined by rehabilitation specialists based on clinical judgment, consistent with routine clinical practice, while cognitive screening through MoCA was used descriptively and for exploratory analyses.

The FMA is a standardized Likert-scale assessment widely used to evaluate motor function recovery following stroke-induced hemiplegia. It assesses multiple domains, including motor function, sensation, range of motion, and joint pain. The upper-

extremity subsection of the FMA (FMA-UE) has a maximum score of 66 points [51]. A minimal clinically meaningful improvement following treatment is typically defined as an increase of +4 to +7 points [52]. The MoCA is a widely used cognitive screening tool designed to assess cognitive impairment. Scores range from 0 to 30, with a score above 26 considered indicative of normal cognitive function [53]. MoCA was administered primarily as a screening tool to ensure that participants were cognitively apt to engage with the VR–BCI training. In addition, given evidence that motor rehabilitation may sometimes be accompanied by secondary cognitive improvements, MoCA scores were also monitored as an exploratory outcome. Finally, data for participants *P40* and *C05* are incomplete (Table 1) due to protocol modifications implemented for the final batch of patients, resulting in the absence of follow-up assessments for both the FMA and MoCA.

2.2.1. Study Design and Protocol Deviations: Randomization used a simple procedure without stratification or blocking. The sequence was generated by one team member and was not concealed; personnel enrolling participants had access, while participants did not. Although the initial trial registration specified single-blinding for the outcomes assessor, no blinding was ultimately implemented due to the nature of the interventions. Furthermore, the Kinesthetic and Visual Imagery Questionnaire (KVIQ) [54] was omitted from the final protocol to reduce participant fatigue. The MoCA and MAS remained the primary longitudinal measures, assessed at baseline, final (4 weeks), and 1-month follow-up.

2.3. Experimental Design

2.3.1. Experimental protocol: The experimental protocol for this study consisted of a 4-week intervention, including a total of 12 VR-BCI training sessions for the experimental group, except for participant P05 with 10 sessions, and participant P40 with 11 sessions. The participants in the control group did not follow the VR-BCI experimental intervention but instead engaged in additional hours of conventional therapy. Clinical evaluations and functional brain imaging assessments were conducted at three distinct time points: (1) before the intervention (pre); (2) immediately after completing the intervention (post); and (3) one month following the intervention (follow-up). Both the BCI training and brain imaging with functional Magnetic Resonance (fMRI) for participants with stroke were carried out at the Central Hospital of Funchal. fMRI data were acquired as part of a parallel investigation and are not reported here, as they fall outside the scope of the present EEG-focused analysis.

For the participants without stroke, a single MI-BCI session was used for this analysis. These sessions took place in a lab environment, in two different physical locations. At the NeurorehabLab of University of Madeira, and the NeuroLab of the Evolutionary Systems and Biomedical Engineering Lab (LaSEEB)/Institute of Systems and Robotics in Lisbon.

Baseline Sensorimotor EEG and Its Longitudinal Change.

2.3.2. EEG and VR equipment: For participants with stroke, EEG data was acquired using the g.Nautilus wireless EEG amplifier (g.tec, Graz, Austria) with 32 channels (Figure 2A), a sampling rate of 500 Hz, and 24-bit resolution. Electrodes were placed according to the 10–10 system, and data was transmitted wirelessly via a 2.4 GHz ISM band to a desktop computer for real-time processing. For participants without stroke, EEG data was recorded using both the g.Nautilus and the Liveamp 32 EEG amplifier (Brain Products GmbH, Munich, Germany), maintaining the same 32-channel setup and 500 Hz sampling rate as the stroke group. Both devices have similar specifications and are functionally equivalent in terms of data acquisition performance and noise characteristics. The main difference lies in the brand rather than technology or configuration. This makes a systematic hardware bias unlikely.

Visual feedback was delivered through the Oculus Rift CV1 (Resolution: 1080x1200 per-eye; Refresh Rate: 90 Hz; field of view (FoV): 87° horizontal, 88° vertical; 6 degrees of freedom (DoF) motion tracking) and the Oculus Quest 2 (Resolution: 1832x1920 per-eye; Refresh Rate: 120 Hz; field of view (FoV): 97° horizontal, 93° vertical; 6 degrees of freedom (DoF) motion tracking) systems (Figure 2B). Additionally, vibro-tactile feedback was provided through two Oculus Touch controllers (Figure 2C) modified with a custom support base for patient comfort (Figure 2D).

Figure 2: VR-BCI Experimental Setup: A. EEG System with 32 electrodes; B. HMD for VR feedback; C. Controllers for vibrotactile feedback; D. Custom controller support; E. MI protocol illustrating the epoch size and visual feedback through NeuRow.

2.3.3. VR-BCI training paradigm and protocol: The VR-BCI training task utilized NeuRow [55], a first-person upper-limb MI and MO paradigm in immersive VR. The

protocol involved MI-MO training through embodied feedback, rendered through a Head-Mounted Display (HMD), with vibro-tactile feedback. Participants were seated in a virtual boat and instructed to perform MI and MO of proximal, rowing movements, guided by an on-screen directional cue (left or right arrow). The avatar's two arms were always visible to preserve ecological context, but only the cued side was to be imagined at each trial. Multimodal feedback was provided: visual feedback depicted the avatar's arm movement in the cued direction; auditory feedback delivered ambient and event-specific sounds (e.g., water splashes, scoring) via the HMD headphones; and vibro-tactile feedback produced brief hand vibrations through the Oculus Touch controller corresponding to the cued side.

The training procedure comprised two phases: (1) Calibration — participants performed cued left- vs right-hand MI synchronized with avatar rowing actions and vibro–tactile cues. Each session included 20 randomized trials per hand, with 2 s of baseline and 4 s of MI (Figure 2E). A randomized inter-trial interval (1.25–1.5 s) was applied to prevent stimulus anticipation and carryover effects. EEG data from calibration were used to extract spatial and spectral features through a common spatial patterns (CSP) filter (4 filters used, in the frequency band of 8 - 30 Hz), which trained a linear discriminant analysis (LDA) classifier, a widely adopted approach for MI-based BCIs [56]. (2) Online training — the trained model then classified MI patterns in real time, enabling participants to control the virtual boat through MI of the cued arm, with the same trial number and duration as in training, and as implemented in previous studies using similar protocols [57]. The same protocol was applied to both stroke and healthy participants.

2.3.4. Design rationale of the NeuRow VR paradigm: NeuRow employs a bimanual design to engage bilateral sensorimotor networks and promote interhemispheric rebalance after stroke by enhancing ipsilesional recruitment, reducing contralesional inhibition, and enabling repetitive, error-reduced practice [58, 59, 60]. To further increase sensorimotor activation, NeuRow combines motor imagery and observation (MIMO), leveraging the mirror neuron and action-observation networks [61, 62, 63], which enhance premotor and parietal activation when imagery and observation are integrated [64, 65]. MIMO-based VR paradigms have shown stronger ERD responses than MI alone [66, 50]. Brain-contingent feedback advances the virtual boat and delivers a co-timed vibrotactile pulse, reinforcing associative (Hebbian) learning and sensorimotor coupling through precise temporal synchronization of visual and tactile feedback with motor intention [67, 68, 69].

2.4. EEG Data Analysis

For the post-hoc analysis, EEG signals were processed using MATLAB R2023a (The MathWorks, MA, United States) and the EEGLAB toolbox v2023.1 [70].

2.4.1. EEG Pre-Processing Optimization in Clinical Settings: Given that our stroke data were recorded in a hospital setting, a naturally higher-noise environment, and involved individuals with brain lesions, we anticipated an increased level of noise compared to standard laboratory conditions. Consequently, EEG pre-processing was a critical aspect of our methodology, requiring careful investigation to ensure optimal signal quality. To address this, we explored and compared multiple pre-processing pipelines, ranging from basic filtering approaches to more robust and aggressive artifact removal methods. The final pipeline was selected based on a systematic evaluation of performance, as outlined in the schematic presented in Figure 3, while the code is available online‡

The selection of the optimal pre-processing pipeline was based on a two-fold evaluation: first, assessing ERD values obtained after applying each pipeline, and second, conducting a manual inspection to ensure effective artifact removal. Given the high prevalence of artifacts in the stroke cohort, *Pipeline 8* was identified as the most suitable approach (Figure 3).

For the non-stroke population, the same comparative analysis was conducted across different pre-processing pipelines. As the data exhibited lower levels of noise, *Pipeline 6* was selected as the most appropriate method.

2.4.2. Pre-processing: For both groups, the EEG data pre-processing from the training session involved band-pass filtering between 1 and 40 Hz; then for correct continuous noisy data and for rejecting bad channels we applied Artifact Subspace Reconstruction (ASR) method [71], in two steps, first to identify and interpolate bad channels, with the following parameters: *'FlatlineCriterion'=10, 'ChannelCriterion'=0.8, 'LineNoiseCriterion'=5, 'Highpass'='off', 'BurstCriterion'='off', 'WindowCritetion'='off', 'BurstRejection'='off', 'Distance'='Euclidian'*, and then to reject bad segments, with the following parameters: *'FlatlineCriterion'='off', 'ChannelCriterion'='off', 'LineNoiseCriterion'='off', 'Highpass'='off', 'BurstCriterion'=20, 'WindowCritetion'=0.5, 'BurstRejection'='on', 'Distance'='Euclidian', 'WindowCriterionTolerances'=[-Inf 8].* ASR is considered the most effective EEG artifact correction and signal reconstruction algorithm available, ensuring minimal information loss [72]. EEG data were subsequently downsampled using the EEGLAB function `pop_resample()`, which applies a built-in anti-aliasing FIR low-pass filter (cutoff just below the new Nyquist frequency) before resampling, ensuring that higher-frequency components were removed and signal integrity preserved. An Independent Component Analysis (ICA) [73] was also performed to remove remaining artifactual components in the EEG signals. ICA was computed on data after rejecting bad segments, and the resulting weights were applied to the data before segment rejection (Figure 3). We used the ICLabel [74] method, which labels components as one of seven categories (brain, muscle, eye, heart, line noise,

‡ `https://github.com/LaSEEB/NeurAugVR/tree/master/preprocessings`. Note: For our analyses, the order of two preprocessing steps—re-referencing and ICA—was adjusted relative to the original pipeline.

channel noise, or other), based on the probability values of each category for a specific component. In our case, we only removed automatically any component classified as "muscle" or "eye" artifact, if the probability values were at least 90%. After this, we used a full-rank re-referencing to common average. Then, in the case of the data from the participants with stroke, we proceeded to bad segment removal, again running ASR to the data, with the parameters: *FlatlineCriterion'='off', 'ChannelCriterion'='off', 'LineNoiseCriterion'='off', 'Highpass'='off', 'BurstCriterion'=20, 'WindowCritetion'='off', 'BurstRejection'='off', 'Distance'='Euclidian'*, and for the data of the participants without stroke, we rejected bad trials. Finally, the data were segmented into epochs corresponding to left-hand and right-hand trials before performing time-frequency analysis.

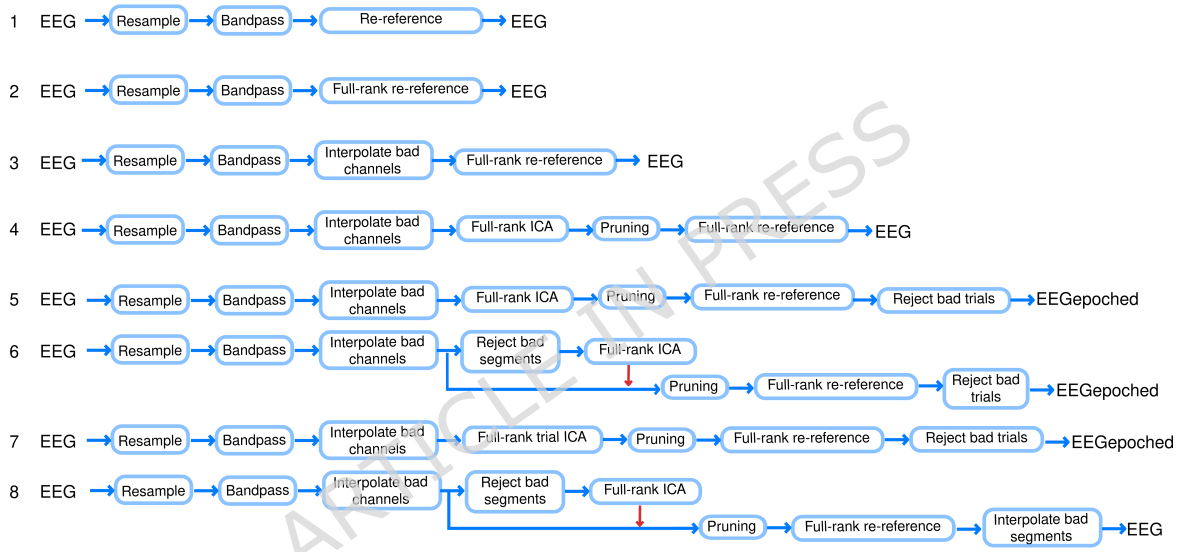

Figure 3: EEG Pre-Processing Pipelines. This schematic illustrates the various EEG processing pipelines tested in the study, ranging from the simplest approach (1) to the most complex method (8). The red arrow in Pipelines 6 and 8 indicates a transfer of weights.

2.4.3. Event-Related Desynchronization (ERD) computation: The ERD values were calculated based on the event-related spectral perturbation (ERSP) values computed using EEGLAB with fixed-window, zero-padded Fast-Fourier Transformations (FFTs) with Hanning taper. The ERSP values are the relative power in decibels (relative to baseline). To transform these values into a percentage decrease, as is normal in the analysis of ERD, we used the following formula:

$$ERD(\%) = (10^{ERSP/10} - 1) \times 100\% \quad (1)$$

Given the variability of ERD values across individuals and even between sessions of the same individual, the use of individualized ERD frequency bands was computed in order to enhance the sensitivity of the ERD analysis to inter-individual neural

dynamics, accounting for post-stroke variability in oscillatory features and frequency shifts that may accompany recovery [68]. Instead of using the conventional 8 – 12 Hz broadband to analyze Alpha oscillations, we determined an individualized frequency band for each participant, electrode, task, and trial. This process began by defining an initial broad frequency range of 6 – 14 Hz. Within the 6–14 Hz range, the spectrum was systematically divided into overlapping frequency bands with a bandwidth of 0.5 Hz (e.g., 6–6.5 Hz, 6.5–7 Hz, etc.). To ensure comprehensive coverage, the segmentation process was repeated with a shifted starting frequency (e.g., beginning at 6.5 Hz instead of 6 Hz), thereby exploring all possible frequency intervals within the target range. For each frequency band, the ERSP was computed, and the mean power value was extracted for subsequent analysis. Finally, we compared the mean power values across all bands and selected the frequency band that yielded the lowest ERSP value. This band was identified as the individualized ERD for the specific participant, electrode, and trial. This can be visualized in Figure 4, and the pseudo-code describing this method is presented in Listing 1, in the Supplementary material. The implementation of this method is available online §.

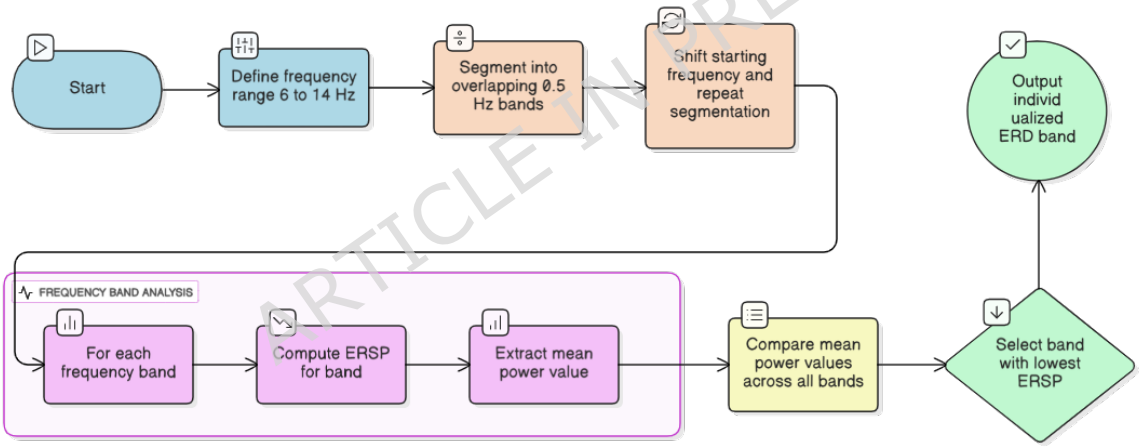

Figure 4: Individualized ERD Computation Flow.

The ERD was extracted from all 32 electrodes, using the same method. Our analysis focused primarily on C3 and C4, as they are positioned over the motor and somatosensory cortices [75]. These electrodes are also the most commonly analyzed in the literature, facilitating comparisons with previous studies [69, 76, 68].

2.4.4. Lateralization Metrics: To quantify interhemispheric asymmetry of sensorimotor activation during motor imagery, two complementary indices were computed: the Lateralization Index (LI) and the Laterality Coefficient (LC).

§ `https://github.com/LaSEEB/Individualized-ERD`

Baseline Sensorimotor EEG and Its Longitudinal Change.

Lateralization Index (LI). The LI was calculated to provide a symmetrical measure of hemispheric differences across left- and right-hand trials [77]. The LI was defined as:

$$LI = \frac{(ERD_{C3}(L) - ERD_{C4}(L)) + (ERD_{C4}(R) - ERD_{C3}(R))}{2}, \tag{2}$$

where $ERD_{C3}(L)$ and $ERD_{C4}(L)$ correspond to the ERD values recorded during left-hand motor imagery, and $ERD_{C3}(R)$ and $ERD_{C4}(R)$ during right-hand imagery. In this formulation, positive LI values indicate stronger right-hemisphere activation, while negative values reflect stronger left-hemisphere activation. However, in participants with stroke, the directionality of LI depends on lesion side, which can obscure group-level effects.

Laterality Coefficient (LC). We additionally computed the LC [27, 78], which expresses hemispheric dominance relative to the affected (contralateral) hand:

$$LC = \frac{C - I}{|C + I|} \tag{3}$$

where C and I denote the mean contralateral and ipsilateral ERD values, respectively, with respect to the lesioned hemisphere. For each participant with stroke, these values were obtained from electrodes C3 and C4 across left- and right-hand trials. For example, for participants with right-hemisphere lesions:

C = mean[ERD(right-hand trial, C3) + ERD(left-hand trial, C3)]

I = mean[ERD(right-hand trial, C4) + ERD(left-hand trial, C4)]

The LC provides a normalized measure of contralateral dominance, allowing direct comparison across lesion sides. Higher LC values reflect stronger contralateral ERD (typical in healthy controls), whereas lower or negative values indicate reduced or reversed lateralization (often observed after stroke).

2.5. Statistical Analyses

All analyses were performed in MATLAB R2023a (The MathWorks, MA, United States) using the Statistics and Machine Learning Toolbox. Linear mixed-effects models (LMEs) were used for both clinical and neurophysiological data to account for repeated measures and inter-individual variability, including random intercepts per participant. Model assumptions were verified using formal statistical tests. Normality was assessed visually through Q–Q plots and formally with the Jarque–Bera test, while homoscedasticity was evaluated using Breusch–Pagan and Levene tests confirming that the residuals met model criteria. Statistical significance was set at two-tailed $p < 0.05$, and all post-hoc pairwise comparisons were Bonferroni-corrected to control for multiple testing within each analysis family. No data imputation was performed; all analyses used available data from participants who completed each assessment.

Baseline Sensorimotor EEG and Its Longitudinal Change.

Given the sample size and the absence of stratified randomization, potential group differences in demographic and clinical characteristics were addressed analytically. Baseline motor impairment was controlled for by including baseline FMA score as a covariate in clinical outcome models, and stroke type (ischemic vs. hemorrhagic) was included as a fixed effect in ERD-related LME models.

2.5.1. Clinical comparisons: An LME was fitted to the data to evaluate the effects of assessment time (Pre, Post, Follow-up) and group (Experimental vs. Control) on FMA scores, while accounting for within-subject variability and baseline motor impairment. The model included Baseline FMA as a covariate and an interaction between Time and Group:

$$\text{FMA\_Score} \sim 1 + \text{Baseline} + \text{Time} * \text{Group} + (1 \mid \text{ID}) \tag{4}$$

This controls for initial differences in FMA between groups, providing baseline-adjusted estimates of time and group effects.

2.5.2. Analysis of ERD: To compare ERD values between participants with stroke and those without stroke, two analytical approaches were employed. (1) A Mann–Whitney U test was used to compare ERD values between the stroke and non-stroke (reference) groups. This non-parametric test was selected due to the small sample sizes and non-normal distribution of the data. The analysis was conducted separately for each session and across all EEG channels. (2) An LME model was used to account for individual variability and to examine ERD differences across sessions.

For the LME, we modeled ERD as a function of training sessions, group (participants with stroke vs. non-stroke), and trial type (Left vs. Right-hand movement), while accounting for individual variability through a random intercept and slope per subject. The model included an interaction term between session progression and trial type to assess whether ERD changes differed based on movement laterality:

$$\text{mean\_erd} \sim 1+\text{group}+\text{sessions}\times\text{trial}+(1+\text{group} \mid \text{subjects})+(1+\text{sessions} \mid \text{subjects}) \tag{5}$$

Finally, Analysis of variance (ANOVA) analysis was used after LME to test the significance of fixed effects.

2.5.3. Analysis of affected side ERD: To further account for the potential confounding effect of lesion laterality, an additional analysis was performed for each participant with stroke relative to the affected side. An LME was fitted exclusively to the stroke cohort to investigate the effects of session progression and hand condition on ERD:

$$mean\_erd \sim 1 + sessions \times affected\_side + (1 + sessions \mid subjects) \tag{6}$$

where *sessions* represented training session number, *affected_side* distinguished paretic from non-paretic trials, and random intercepts and slopes were included per subject.

Baseline Sensorimotor EEG and Its Longitudinal Change.

2.5.4. Analysis of Lateralization Metrics: To examine changes in lateralization over time and their relationship to group differences, we modeled LI and LC as a function of session (representing progression over time) and group (stroke vs. non-stroke participants). Individual variability was accounted for by including random intercepts and slopes for each subject:

$$\text{li} \sim 1+\text{sessions}+\text{group}+(1+\text{group} \mid \text{subjects})+(1+\text{sessions} \mid \text{subjects}) \quad (7)$$

$$\text{lc} \sim 1+\text{sessions}+\text{group}+(1+\text{group} \mid \text{subjects})+(1+\text{sessions} \mid \text{subjects}) \quad (8)$$

This allowed us to examine whether laterality changed over time (sessions), whether differences existed between groups (participants with stroke vs. non-stroke), and whether these effects varied between individuals.

2.5.5. Two-Stage Linear Modeling of ERD to Predict Motor Recovery: To examine the relationship between longitudinal predictors (ERD progression across training sessions) and cross-sectional clinical outcomes (ΔFMA), we implemented a two-stage modeling approach, following methods used in previous studies [68, 79]. LME models were selected because they provide robust regression estimates while accounting for subject-specific variability [80].

In the first stage, an LME model was fitted to estimate individual ERD trajectories (from the affected side) over the intervention period using the following formula:

$$\text{mean\_erd} \sim \text{sessions} \times \text{stroke\_type} + (\text{sessions} \mid \text{subjects}) \quad (9)$$

This model included time (sessions) and subjects as random effects, allowing patient-specific variability in both initial/baseline ERD values (intercept) and their progression over time (slope). The intercept and slope extracted represent the baseline ERD level of each participant and their rate of change in ERD throughout the intervention.

In the second stage, the extracted ERD *intercepts* and *slopes* were then incorporated into a linear regression model to predict clinical motor recovery, measured by ΔFMA:

$$\text{delta\_fma} \sim \text{slope} \times \text{intercept} \quad (10)$$

3. Results

3.1. Clinical Outcome

The baseline-adjusted LME was used to assess the effects of time (Pre, Post, Follow-up) and group (Experimental vs. Control) on motor recovery, measured by the FMA (Figure 5). This model included baseline FMA (centered) as a covariate to control for initial differences between groups and a random intercept for each participant to account for within-subject variability.

The analysis revealed a significant main effect of Time on FMA scores. Participants showed clear motor improvements from Pre to Post ($\beta = 5.80$, $p = 0.017$) and from Pre

to Follow-up ($\beta = 10.11$, $p < 0.001$), indicating sustained functional gains beyond the intervention period. Baseline FMA was a strong positive predictor of overall scores ($\beta = 0.98$, $p < 0.001$). In contrast, the main effect of Group (Experimental vs. Control; $\beta = 0.33$, $p = 0.91$) and the Time × Group interactions were not statistically significant, although the Follow-up × Group interaction approached significance ($\beta = -6.20$, $p = 0.056$).

Between-group contrasts confirmed no significant difference at Post ($p = 0.61$) and a trend at Follow-up ($p = 0.06$). These findings indicate that both groups demonstrated comparable improvement trajectories after accounting for baseline differences in motor function (Table 2).

Table 2: Fixed and random effects estimates from the Linear Mixed-Effects Model (LME) analyzing FMA scores (baseline-adjusted). The model included baseline FMA (centered) as a covariate and an interaction between Time and Group. The 95% confidence intervals (CIs) provide a measure of estimate uncertainty.

Fixed Effects	**Estimate (β)**	**95% CI (Lower, Upper)**	**t-Stat**	**p-Value**
Intercept	35.92	[31.52, 40.31]	16.70	< 0.001
Time: Post vs. Pre	5.80	[1.11, 10.49]	2.53	0.017
Time: Follow-up vs. Pre	10.11	[5.06, 15.16]	4.09	< 0.001
Group (Experimental vs. Control)	0.33	[–5.43, 6.09]	0.12	0.91
Baseline FMA (centered)	0.98	[0.84, 1.12]	14.42	< 0.001
Time (Post) × Group (Experimental)	–1.80	[–7.77, 4.17]	–0.62	0.54
Time (Follow-up) × Group (Experimental)	–6.20	[–12.56, 0.16]	–1.99	0.056
Random Effects Variance (σ^2)		**95% CI (Lower, Upper)**		
Subjects (Intercept)		[1.56, 5.34]		
Residual Error		[2.74, 4.81]		

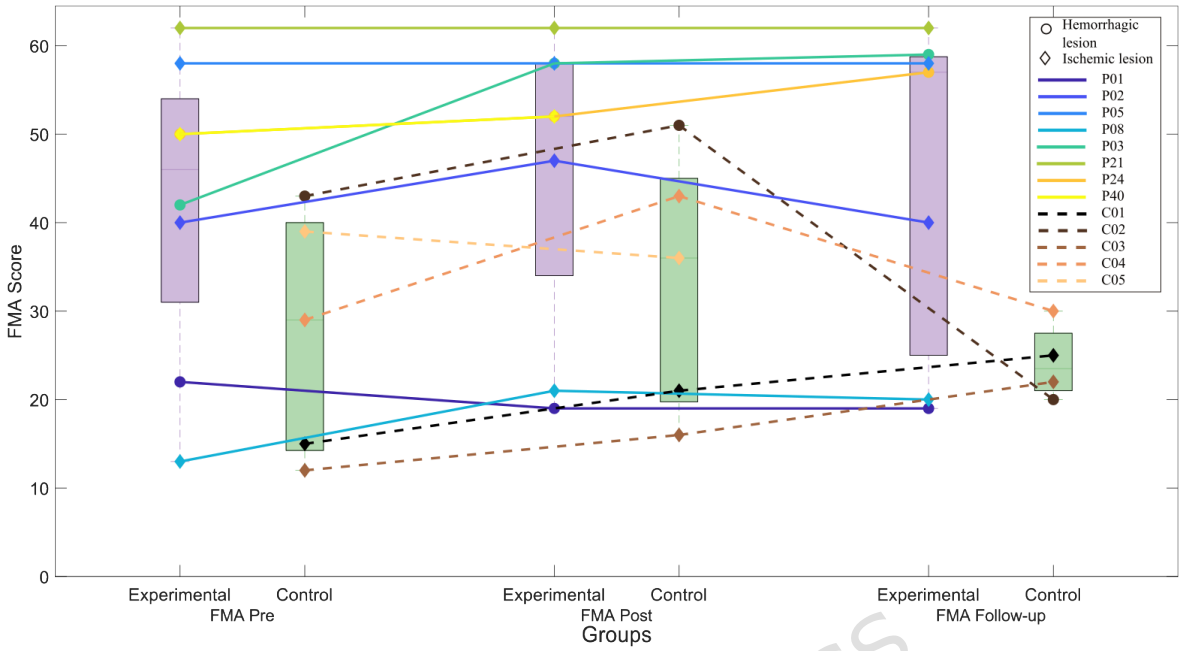

Figure 5: FMA Scores. Individual trajectories for each participant are displayed, with solid lines representing the experimental group and dashed lines representing the control group. Colors distinguish participants, and lesion type (hemorrhagic or ischemic) is indicated by different markers. Patient P40 does not have a follow-up value, since this was not acquired.

3.2. Neurophysiological Outcomes

3.2.1. Comparison of ERD Spatial Distribution: The ERD responses of participants with stroke were compared to those of the non-stroke group, which served as a reference cohort, to assess differences in neural activity patterns. Figure 6 illustrates the spatial distribution of the mean ERD, including aggregated ERD values across all sessions for participants with stroke, divided into the participants with paretic hand and non-paretic hand relevant to the specific trial (right- or left-hand), and the mean ERD of the non-stroke group. The Mann-Whitney U-test revealed significant differences in ERD between groups for Left-hand trials: if the paretic hand was the right, then it was significant at five electrode sites: C3 ($U = 1647$, $p = 0.00178$), C4 ($U = 1663$, $p = 0.000799$), CP1 ($U = 1064$, $p = 0.0321$), CP2 ($U = 1087$, $p = 0.0173$), and P3 ($U = 1264$, $p = 0.009$); if the paretic hand was the left, then it was significant at three electrode sites: C4 ($U = 3136$, $p = 0.0031$), T8 ($U = 3017$, $p = 0.0127$), and CP6 ($U = 2604$, $p = 0.0433$). For Right-hand trials: if the paretic hand was the right, a significant difference was observed at four electrode sites: C3 ($U = 1659$, $p = 0.000978$), CP5 ($U = 949$, $p = 0.00644$), CP1 ($U = 1073$, $p = 0.0201$), and P3 ($U = 1258$, $p = 0.0132$); if the paretic hand was the left there was no significant difference observed.

Baseline Sensorimotor EEG and Its Longitudinal Change.

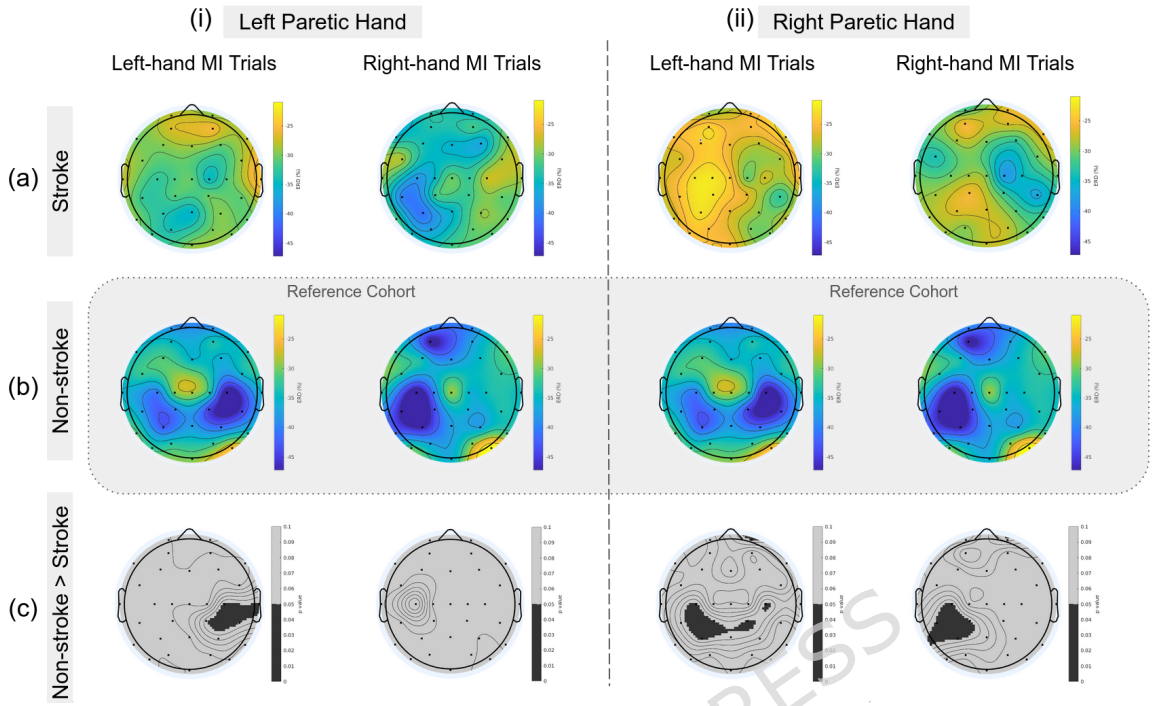

Figure 6: Comparison of ERD topographies between participants with stroke and non-stroke controls. Panels (a) and (b) show the spatial distribution of mean ERD during left- and right-hand motor imagery (MI) trials for participants with stroke (a) and the non-stroke reference cohort (b). The data are organized by the side of the paretic hand: (i) left paretic hand and (ii) right paretic hand. Warm colors indicate stronger ERD (greater desynchronization), while cool colors indicate weaker ERD. Panel (c) displays the Mann–Whitney U-test p-value maps comparing the two groups (contrast: non-stroke $>$ stroke), with darker areas representing significant differences ($p < 0.05$, Bonferroni corrected for multiple comparisons).

3.2.2. Modeling ERD Dynamics: Initially, the LME analysis revealed that participants with stroke exhibited significantly reduced ERD compared to the non-stroke group ($\beta = -6.63$, $p = 0.022$). However, no significant change in ERD was observed over time ($\beta = -0.13$, $p = 0.721$), indicating that ERD remained relatively stable throughout the training period (Figure 7 and Figure 8). Furthermore, analysis of hemispheric lateralization revealed no significant changes across sessions for either the LI or the LC. However, a significant group effect was found for LI ($\beta = 8.93$, $p = 0.020$), with participants with stroke showing greater variability and reduced lateralization stability compared to the non-stroke group (Table 5). The LC showed a similar but non-significant trend toward lower values in the stroke cohort ($\beta = -0.11$, $p = 0.066$), suggesting weaker contralateral dominance relative to healthy controls (Table 6).

Finally, the ANOVA results confirmed a significant main effect of group ($F = 5.29$, $p = 0.032$), reinforcing that ERD differences between stroke and non-stroke participants were consistent. However, session progression ($F = 0.13$, $p = 0.726$), trial type

($F = 0.34$, $p = 0.560$), and their interaction ($F = 0.30$, $p = 0.583$) did not reach statistical significance, indicating that ERD changes were not systematically influenced by time or movement laterality (Table 3).

Table 3: Fixed and random effects estimates from the Linear Mixed-Effects Model (LME) analyzing ERD progression. The table reports estimated coefficients (β) for fixed effects, standard errors (SE), 95% confidence intervals (CIs), t-statistics, and corresponding p-values. Variance components (σ^2) for random effects are also presented.

Fixed Effects	**Estimate (β)**	**95% CI (Lower, Upper)**	**t-Stat**	**p-Value**
Intercept	-18.42	[-23.41, -13.43]	-7.27	4.67×10^{-12}
Sessions	-0.13	[-0.85, 0.59]	-0.49	0.721
Group (Stroke vs. Control)	-6.63	[-12.32, -0.95]	-2.30	0.022
Trial (Right vs. Left)	-1.18	[-5.18, 2.81]	-0.58	0.560
Sessions × Trial	-0.18	[-0.83, 0.47]	-0.55	0.583
Random Effects	**Variance (σ^2)**	**95% CI (Lower, Upper)**		
Patient ID (Intercept)	3.91	–		
Group Variance	9.94	–		
Session Variance	0.68	–		
Residual Error Variance	9.88	–		

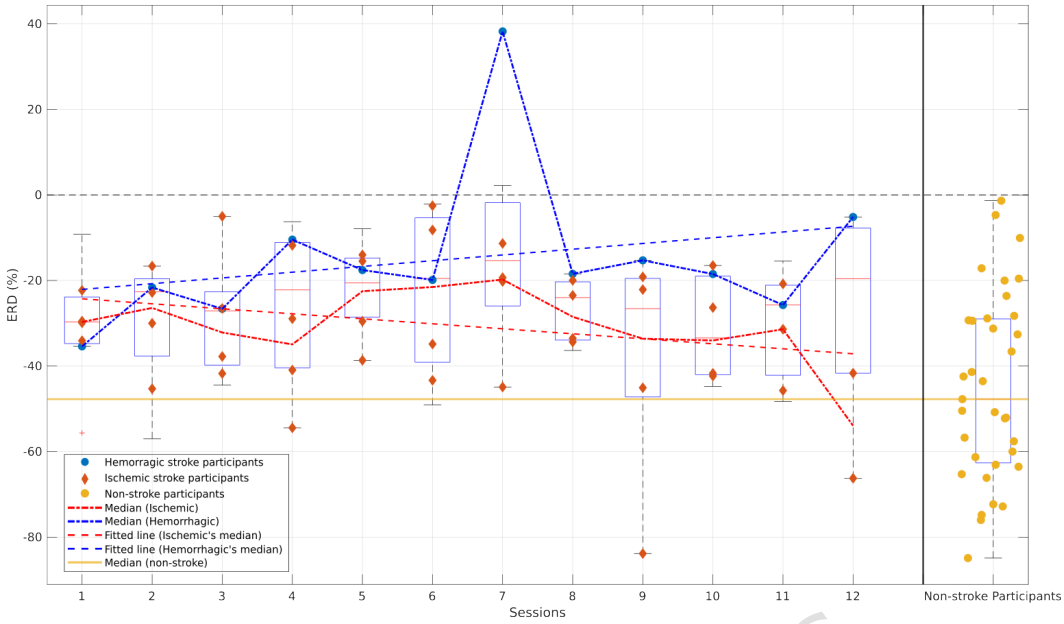

(a) Paretic Side.

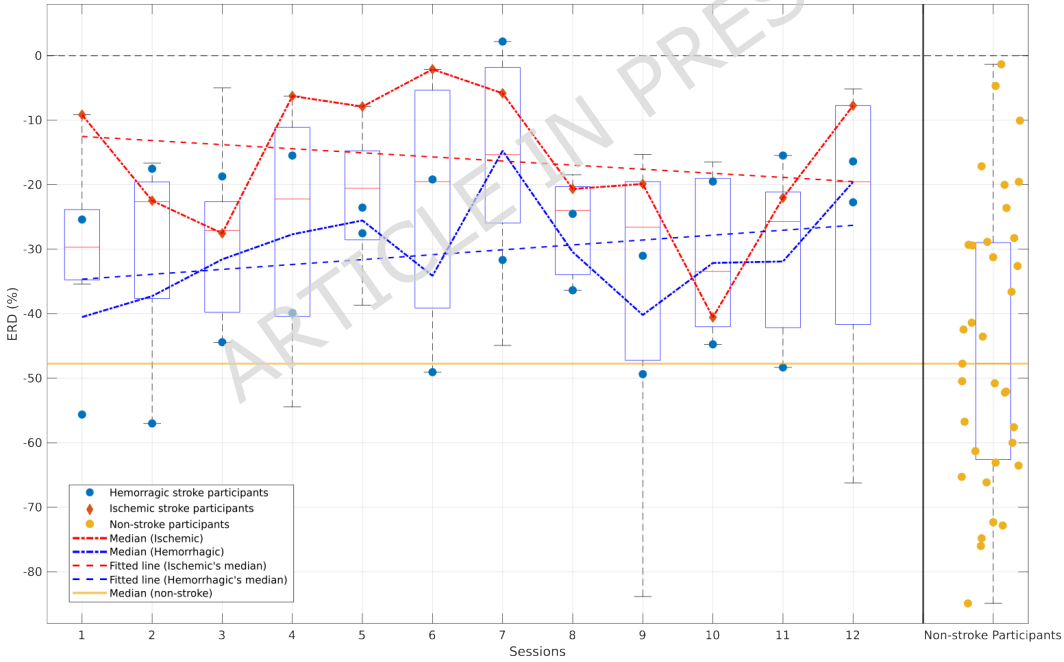

(b) Non-paretic Side.

Figure 7: Left-trials ERD from participants with stroke across sessions vs non-stroke participants, contralateral analysis (C4). The figure is divided into (a) ERD from stroke participants, in which the paretic side is the left; and (b) ERD from stroke participants which the non-paretic side is the left. In both plots, we show two lines for each of the ERD median and fitted lines, for hemorrhagic stroke (blue) and ischemic stroke (red); in yellow, we plotted the median of the non-stroke participants for easier comparison. For each session, the participants with stroke are identified as hemorrhagic (blue) and ischemic (red).

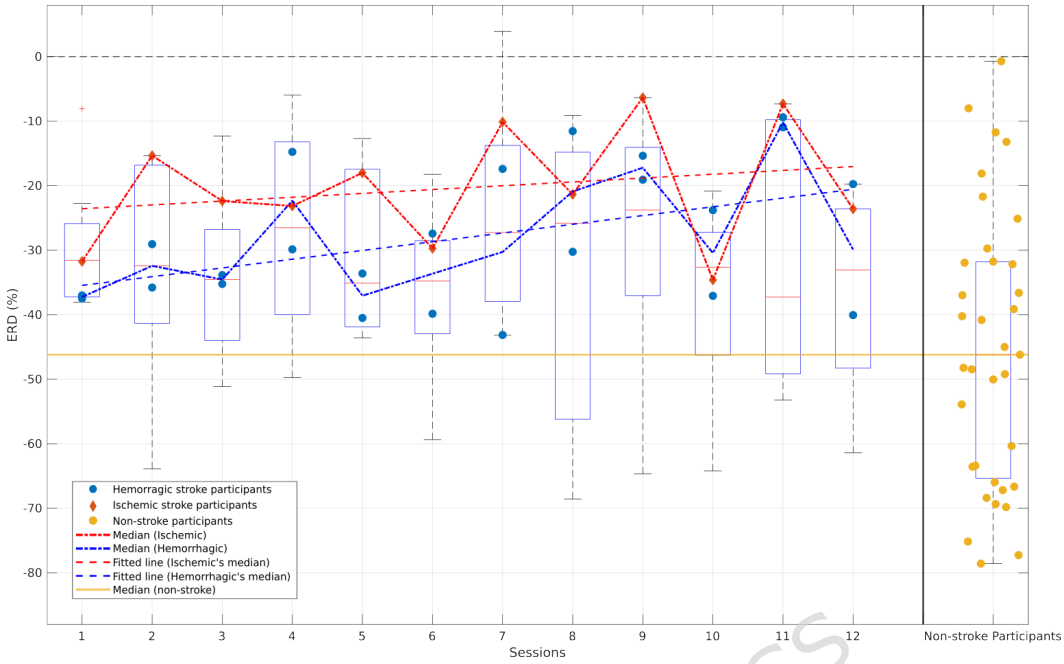

(a) Paretic Side.

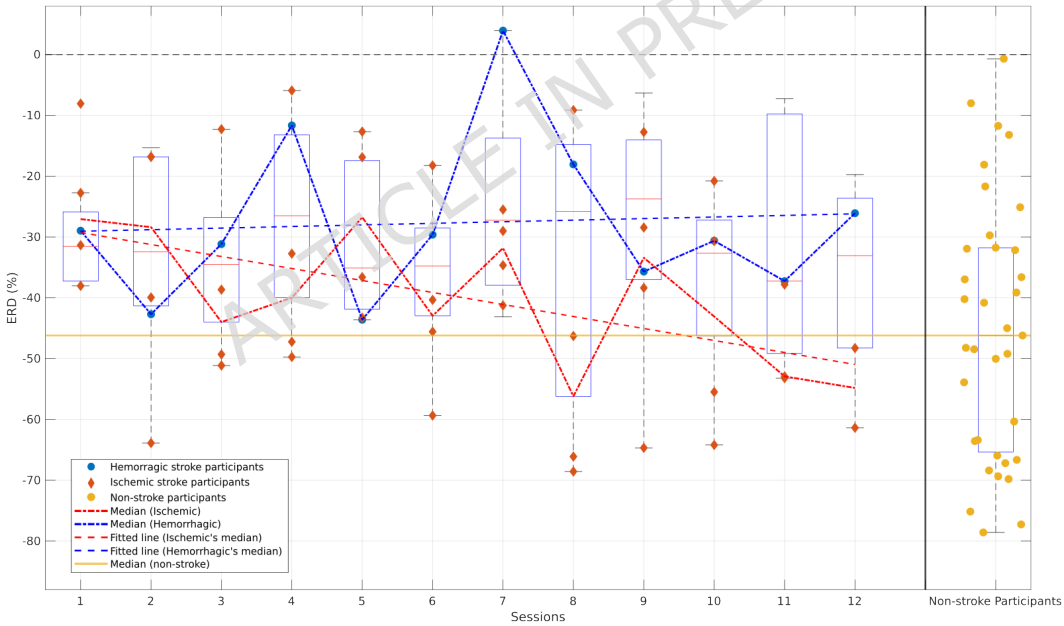

(b) Non-paretic Side.

Figure 8: Right-trials ERD from participants with stroke across sessions vs non-stroke participants, contralateral analysis (C3). The figure is divided into (a) ERD from stroke participants, in which the paretic side is the right, and (b) ERD from stroke participants which the non-paretic side is the right. In both plots, we show two lines for each of the ERD median and fitted lines, for hemorrhagic stroke (blue) and ischemic stroke (red); in yellow, we plotted the median of the non-stroke participants for easier comparison. For each session, the participants with stroke are identified as hemorrhagic (blue) and ischemic (red).

Baseline Sensorimotor EEG and Its Longitudinal Change.

3.2.3. ERD Analysis Aligned to the Affected Hand: To account for differences between affected and unaffected hemispheres, ERD data were re-aligned according to each stroke participant's affected hand. The LME model revealed no significant main effect of session ($F(1, 14.29) = 1.29$, $p = 0.27$), nor of hand condition ($F(1, 170.42) = 0.005$, $p = 0.95$), and the interaction between session and hand condition was also non-significant ($F(1, 170.42) = 1.84$, $p = 0.18$). Model fit indices indicated adequate convergence ($AIC = 1525.1$, $BIC = 1550.9$). These results suggest that ERD amplitude remained stable across sessions and did not differ significantly between paretic and non-paretic hands (Table 4).

Table 4: Linear Mixed-Effects Model results for ERD aligned to the affected (paretic) hand in stroke participants.

Fixed Effect	**Estimate (β)**	**SE**	**t**	**DF**	**p-Value**	**95% CI (Lower, Upper)**
Intercept	-27.67	4.17	-6.64	182	< 0.001	[-35.89, -19.45]
Sessions	-0.66	0.58	-1.14	182	0.257	[-1.80, 0.49]
Paretic hand	0.27	4.05	0.07	182	0.946	[-7.71, 8.26]
Sessions × Paretic hand	0.76	0.56	1.35	182	0.177	[-0.35, 1.88]
Model fit:	AIC = 1525.1, BIC = 1550.9, Log-likelihood = -754.57, Deviance = 1509.1					

3.2.4. Modeling Lateralization Dynamics: In terms of LI, the model demonstrated good overall fit ($AIC = 1014$, $BIC = 1042.5$). No significant main effect of session was observed ($\beta = 0.042$, $p = 0.904$), indicating that LI remained stable across the 12 training sessions. However, a significant group effect emerged ($\beta = 8.93$, $p = 0.020$), with stroke participants showing higher LI variability compared to the non-stroke group (Figure 9). This suggests that while interhemispheric balance remained relatively constant over time, stroke participants exhibited overall reduced lateralization stability, consistent with altered hemispheric activation following stroke. Random effects analysis indicated moderate inter-individual variability in baseline LI values ($\sigma^2_{intercept} = 1.33$) (Table 5).

Table 5: Linear Mixed-Effects Model results for Lateralization Index (LI).

Fixed Effect	**Estimate (β)**	**SE**	**t**	**DF**	**p-Value**	**95% CI (Lower, Upper)**
Intercept	2.873	2.219	1.29	125	0.198	[-1.519, 7.266]
Sessions	0.042	0.349	0.12	125	0.904	[-0.648, 0.732]
Group (control)	8.932	3.776	2.37	125	0.020	[1.459, 16.406]
Model fit:	AIC = 1014, BIC = 1042.5, Log-likelihood = -497.00, Deviance = 993.99					

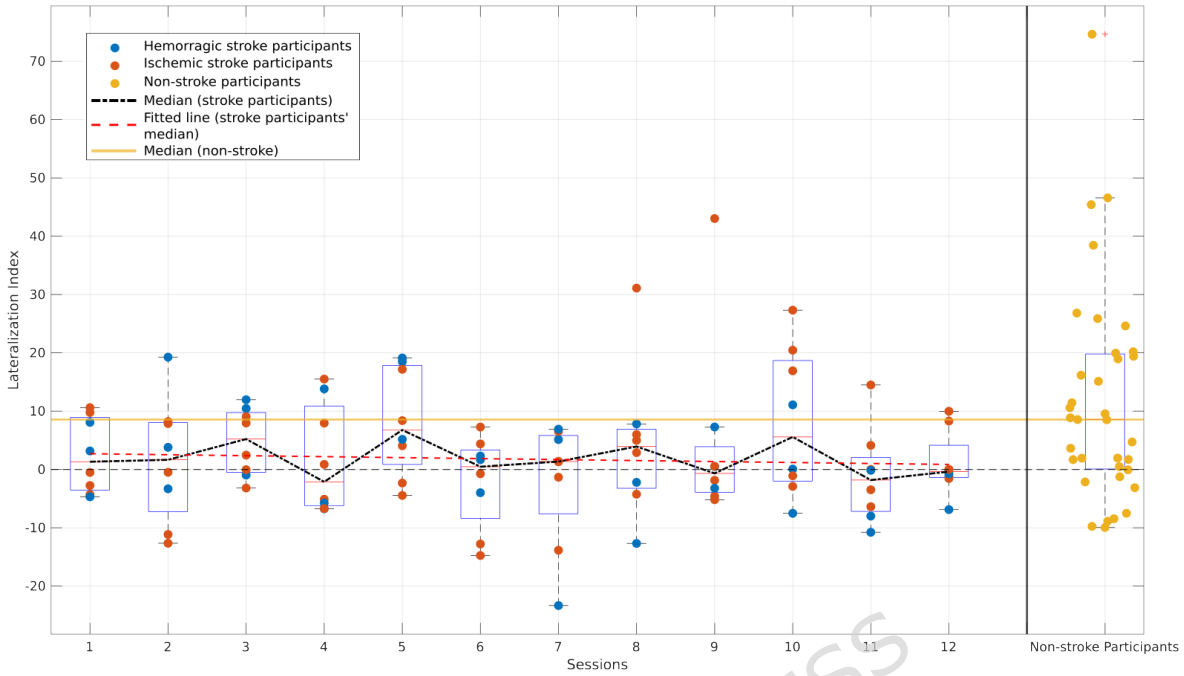

Figure 9: Lateralization Index of participants across sessions. We distinguish participants with stroke between type of stroke: hemorrhagic (blue) and ischemic (red). In the plot, we also show a line connecting the median of the participants with stroke for all sessions (dashed black) and a fitted line for the same median (dashed red).

In terms of LC, no significant effect of session was found ($\beta = 0.003$, $p = 0.701$), indicating that LC remained stable throughout the 12 training sessions. The group effect approached significance ($\beta = -0.111$, $p = 0.066$), suggesting a trend toward lower LC values in participants with stroke compared to controls, consistent with reduced contralateral dominance (Figure 10). Random effects analysis showed minimal between-subject variance, indicating that individual LC trajectories were relatively homogeneous across participants (Table 6).

Table 6: Linear Mixed-Effects Model results for Laterality Coefficient (LC).

Fixed Effect	**Estimate (β)**	**SE**	**t**	**DF**	**p-Value**	**95% CI (Lower, Upper)**
Intercept	0.0479	0.0515	0.93	125	0.354	[-0.054, 0.150]
Sessions	0.0031	0.0080	0.39	125	0.701	[-0.013, 0.019]
Group (control)	-0.1112	0.0599	-1.86	125	0.066	[-0.230, 0.007]
Model fit:	AIC = 14.06, BIC = 42.58, Log-likelihood = 2.97, Deviance = -5.94					

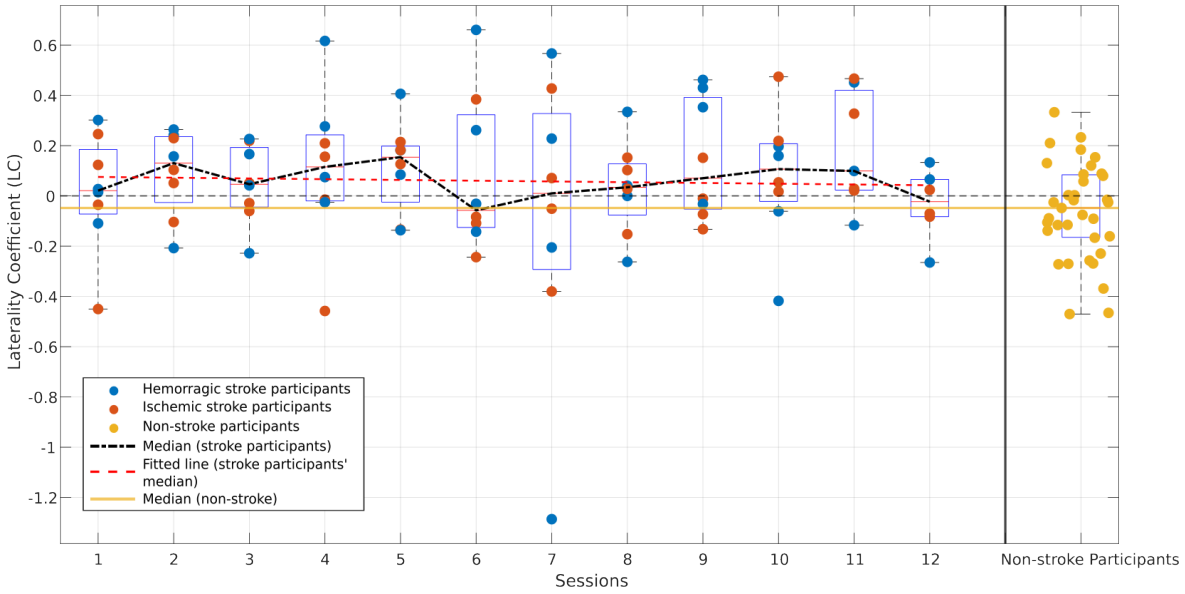

Figure 10: LC of participants across sessions. We distinguish participants with stroke between type of stroke: hemorrhagic (blue) and ischemic (red). In the plot, we also show a line connecting the median of the participants with stroke for all sessions (dashed black) and a fitted line for the same median (dashed red). In yellow, we plotted the median of the non-stroke participants.

3.3. Relationship Between ERD Progression and Motor Recovery

The LME analysis revealed a significantly negative intercept ($\beta = -24.692$, $p < 0.001$), indicating that ERD was strongly suppressed across participants. Neither session progression ($\beta = -0.575$, $p = 0.371$) nor stroke type ($\beta = -7.653$, $p = 0.235$) showed significant main effects, suggesting stable ERD patterns over time and similar overall levels between ischemic and hemorrhagic stroke participants. The interaction between session and stroke type was also non-significant ($\beta = 1.925$, $p = 0.061$), though it suggested a potential trend toward distinct ERD trajectories across stroke subtypes.

Random effects indicated notable between-subject variability in baseline ERD ($\sigma^2 = 4.213$), while session-related variability ($\sigma^2 = 0.890$) was smaller, suggesting that inter-individual differences contributed more strongly to ERD variability than session-to-session changes (Table 7). Overall, ERD remained stable across training, with a tendency for stroke type to influence its temporal evolution.

Table 7: Fixed and random effects estimates from the Linear Mixed-Effects Model (LME) analyzing ERD progression over sessions and stroke types.

Fixed Effects	**Estimate (β)**	**95% CI (Lower, Upper)**	**t-Stat**	**p-Value**
Intercept	-24.692	[-32.586, -16.798]	-6.215	1.614×10^{-8}
Sessions	-0.575	[-1.845, 0.696]	-0.899	0.371
Stroke Type	-7.653	[-20.379, 5.073]	-1.195	0.235
Sessions × Stroke Type	1.925	[-0.092, 3.941]	1.897	0.061
Random Effects	**Variance (σ^2)**	**95% CI (Lower, Upper)**		
Subjects (Intercept)	4.213	[0.405, 43.824]		
Sessions (Slope)	0.890	[0.251, 3.155]		
Residual Error	12.37	[10.558, 14.493]		

The second-stage linear regression model tested whether ERD progression (slope) and baseline ERD (intercept) predicted motor recovery (ΔFMA). The model explained 86.8% of the variance in motor recovery ($R^2 = 0.868$, adjusted $R^2 = 0.769$), with a significant overall model fit ($F = 8.78, p = 0.0311$) (Figure 11). These results are summarized in Table 8.

Table 8: Fixed and random effects estimates from the second-stage regression model, linking ERD slopes to FMA score.

Fixed Effects	**Estimate (β)**	**95% CI (Lower, Upper)**	**t-Stat**	**p-Value**
Intercept	-36.563	–	-1.3166	0.25833
Slope	62.172	–	2.404	0.074031
Intercept (Baseline ERD)	-1.6006	–	-1.4881	0.21094
Slope × Intercept	2.446	–	2.4985	0.066875
Model Performance			R^2	**p-Value**
All Participants			0.868	0.0311

When analyzing stroke subtypes separately, the relationship between ERD progression and motor improvement differed (Figure 11). Across all participants, the relationship was negative but not statistically significant ($R = -0.680$, $p = 0.063$). For hemorrhagic stroke participants, the relationship was stronger but remained non-significant ($R = -0.926$, $p = 0.246$). For ischemic stroke participants, no meaningful relationship was found ($R = 0.441$, $p = 0.457$).

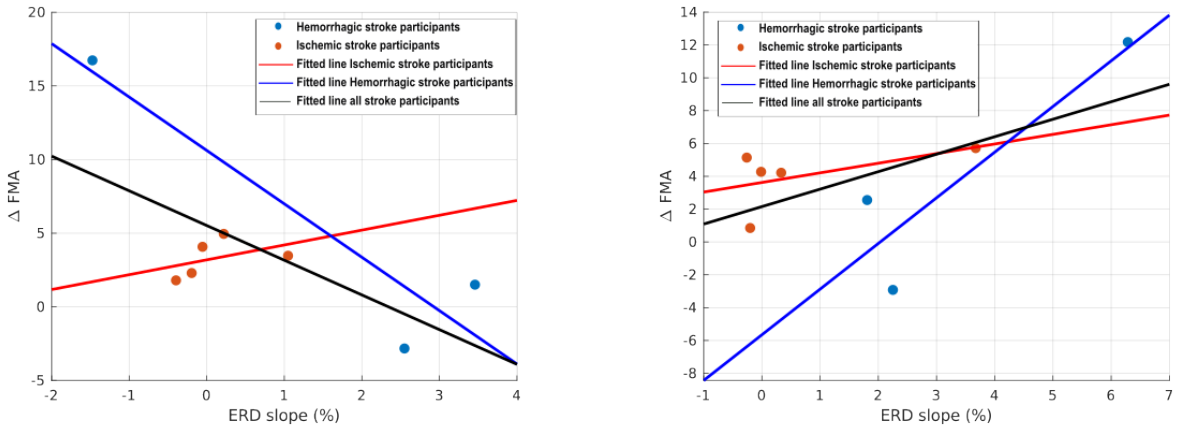

(a) (b)

Figure 11: Linear model predicting the clinical improvement (ΔFMA) on the lesioned (a) and healthy hemispheres (b) of all participants with stroke. We show the relationship between the ERD slope (ERD progression) and the motor function improvement (ΔFMA). Blue dots correspond to hemorrhagic stroke, and red to ischemic stroke. For each graph we show the linear fit of all stroke types (black line), of only the hemorrhagic stroke (blue line), and of only the ischemic stroke (red line).

4. Discussion

4.1. Clinical Implications of VR-BCI Intervention

The baseline-adjusted LME model confirmed significant improvements in motor function over time for both the experimental (VR-BCI) and control groups. After controlling for initial FMA differences, no significant group effect or Time × Group interaction was found, indicating that both groups exhibited comparable recovery trajectories. The trend toward a greater improvement in the experimental group at follow-up ($p \approx 0.06$) suggests a possible longer-term benefit that warrants investigation in a larger, balanced sample.

Although both groups demonstrated significant improvement in motor outcomes over time, the absence of a statistically significant group effect indicates that these changes likely reflect general rehabilitation-related recovery processes. This finding is consistent with previous studies showing that motor recovery can continue at chronic stages through repetitive and intensive training, regardless of the feedback modality [4, 81].

MoCA scores showed minor decreases in some participants post-intervention. These variations were not clinically meaningful and are most likely attributable to test–retest variability, fatigue, or unrelated individual factors.

The random effects analysis revealed substantial inter-individual variability, emphasizing that some participants responded more favorably to training than others. This variability is expected in stroke neurorehabilitation, where multiple factors,

including lesion location, stroke chronicity, and baseline motor function, may influence recovery trajectories.

4.2. Neurophysiological Findings

When ERD patterns were compared between participants with stroke and the non-stroke reference group, distinct group differences emerged at specific sensorimotor and parietal electrodes. For participants with stroke whose paretic hand was on the right, significant ERD reductions relative to controls were observed over contralateral and bilateral sensorimotor areas (C3, C4, CP1, CP2, and P3) during left-hand trials, and at C3, CP5, CP1, and P3 during right-hand trials. In contrast, when the paretic hand was on the left, significant differences were restricted to electrodes over the contralesional hemisphere (C4, T8, and CP6) during left-hand trials, with no significant effects during right-hand trials. These results indicate that ERD suppression was generally weaker and more spatially diffuse in stroke participants compared to non-stroke, particularly over central and parietal regions contralateral to the paretic hand.

LME analysis revealed no significant main effect of session progression, suggesting that ERD remained stable throughout the intervention. This contrasts with previous studies indicating progressive ERD suppression with motor learning [35], potentially due to individual variability in response to BCI training or the limited number of sessions. However, the group effect approached statistical significance, suggesting a trend whereby participants with stroke exhibited reduced ERD compared to non-stroke individuals. This aligns with previous findings indicating that stroke-related disruptions in motor networks may reduce ERD magnitude, although this effect is highly variable across individuals [76, 82].

Further, when ERD was re-aligned to each participant's affected hand, the analysis similarly revealed no significant differences between paretic and non-paretic trials, nor any significant interaction with session progression. This indicates that the absence of ERD modulation was not driven by inconsistencies related to lesion laterality or anatomical side labeling. Instead, ERD patterns appeared stable across training sessions regardless of the affected side, suggesting that neural engagement during VR–BCI training was broadly bilateral.

Regarding hemispheric asymmetry, the laterality analyses revealed complementary insights. The LI model showed no significant effect of session but a significant group effect, with participants with stroke exhibiting higher LI variability and overall reduced lateralization stability compared to the control group. This indicates altered interhemispheric dynamics and weaker contralateral dominance in the stroke cohort. Consistent with this, the LC, which normalizes contralateral and ipsilateral ERD relative to the affected hand, did not change significantly across sessions but showed a trend toward lower LC values in the stroke group. This pattern suggests diminished contralateral ERD dominance relative to non-stroke participants, aligning with cortical reorganization mechanisms previously described after stroke [78, 28]. Together,

these findings point to a stable but weakened interhemispheric balance in the stroke population, possibly reflecting compensatory or bilateral recruitment of sensorimotor areas.

The observed variability across participants may be partly explained by differences in lesion location and chronicity. For example, prior work has shown that individuals with subcortical strokes exhibit less pronounced ERD asymmetry, reflecting preserved cortical structures but altered network-level connectivity [82, 23]. Given that most participants in the present study presented with mixed cortical–subcortical lesions, the reduced lateralization likely reflects these broader network-level disruptions rather than purely cortical deficits. While increased contralesional activation could be interpreted as maladaptive plasticity [83], the overall absence of strong asymmetry and limited motor improvement in this cohort do not support this interpretation.

Overall, the absence of significant ERD modulation across sessions and the weak laterality effects should be interpreted with caution. Beyond inter-individual variability and limited training duration, these results may also reflect intrinsic characteristics of the NeuRow VR paradigm. The bimanual and visually immersive design likely promotes distributed, bilateral cortical activation that enhances engagement but may reduce the measurable unimanual ERD modulation typically reported in simpler paradigms. Furthermore, while the LI and LC provide complementary perspectives on hemispheric asymmetry, their stability across sessions may reflect a broader pattern of bilateral cortical engagement during immersive VR–BCI training.

4.3. ERD Dynamics and Motor Recovery

To investigate the relationship between ERD dynamics and motor recovery, we employed a two-stage modeling approach, following previous studies [68, 79].

The regression analysis identified a significant negative intercept, indicating that baseline ERD levels were predictive of motor recovery. While ERD slope was not significantly associated with FMA change, exploratory trends suggest that reductions in ERD over time may be linked to clinical improvement. This suggests that motor recovery may be linked to progressive ERD suppression, a pattern commonly observed in successful motor learning and stroke recovery [35, 68].

Importantly, stroke subtype analyses revealed distinct trends. In the hemorrhagic stroke subgroup, a negative relationship between ERD slope and ΔFMA was observed, whereas in the ischemic stroke subgroup, no clear relationship emerged. Trends suggest that stroke pathology may influence ERD evolution, though statistical significance was not reached. This indicates that other factors, such as lesion location or training intensity, may contribute more significantly to ERD changes. Therefore, further investigation is needed to determine whether different rehabilitation strategies should be tailored based on lesion type.

Finally, when analyzing ERD from the ipsilateral hemisphere (non-lesioned side), an inverse relationship emerged, where greater clinical improvement correlated with

increasing ipsilateral ERD. Notably, this trend became statistically significant in the ischemic stroke group, suggesting that ipsilateral motor cortex activity may play a compensatory role in recovery for this population. These findings support previous studies demonstrating the importance of ipsilateral cortical recruitment in stroke recovery, particularly for individuals with extensive contralateral damage [68].

4.4. Limitations and Future Directions

The findings of this study must be interpreted in light of several limitations. First, the sample size was small, limiting statistical power and the ability to generalize findings. Although the statistical model controlled for baseline FMA to mitigate initial between-group differences, the small and unbalanced sample size limits statistical power and generalization. Future studies with larger cohorts should further validate whether the observed follow-up trend reflects a meaningful treatment effect. Further, the observed trends in ERD progression and motor recovery may become statistically significant in larger cohorts, warranting replication in future studies.

Further, stroke severity, lesion characteristics, and post-stroke duration varied across participants, introducing heterogeneity that may have influenced results. Future research should incorporate detailed neuroimaging assessments to better classify lesion locations and network-level disruptions affecting ERD generation.

Moreover, the study's intervention period (12 sessions) may have been too short to capture long-term neural reorganization. Given that ERD changes can take weeks or months to consolidate, longer-duration studies are needed to assess whether progressive ERD modulation translates to sustained functional improvements.

Finally, the EEG data were acquired using two high-quality systems with comparable specifications and active electrodes, while hardware-related effects are unlikely, this potential source of variability cannot be entirely excluded.

5. Conclusion

This study provides valuable insights into the dynamics of ERD and their relationship with motor recovery following immersive VR-BCI training in individuals with chronic stroke. Although ERD did not significantly change across sessions, participants with stroke exhibited reduced ERD compared to the non-stroke group. Importantly, baseline ERD levels predicted subsequent motor improvement, suggesting their potential as EEG biomarkers of recovery capacity. Furthermore, ipsilateral ERD may play a compensatory role, particularly in individuals with ischemic stroke.

The absence of significant session effects underscores the complexity of post-stroke neural reorganization and highlights the need for larger-scale, individualized rehabilitation studies. Importantly, this work builds upon more than a decade of continuous research using one of the first clinically implemented immersive VR-BCI systems. By maintaining a consistent experimental paradigm, feedback design, and

analysis pipeline, this research line addresses the well-known lack of methodological homogeneity across BCI studies, ensuring reproducibility and comparability of results over time.

Future research should extend these findings by employing longer and more intensive interventions, integrating multimodal neuroimaging to elucidate the mechanistic role of ERD in motor recovery, and validating predictive EEG biomarkers in larger cohorts. Despite current limitations, this study contributes to the growing body of evidence supporting the use of EEG-based neural features to monitor and personalize neurorehabilitation strategies in stroke recovery.

Acknowledgments

This work is supported by the LARSyS - FCT Project (DOI: 10.54499/LA/P/0083/2020, 10.54499/UIDP/50009/2020, and 10.54499/UIDB/50009/2020), the NeurAugVR (PTDC/CCI-COM/31485/2017), the NOISyS project (DOI: 10.54499/2022.02283.PTDC), the NOVA LINCS (DOI: 10.54499/UIDB/04516/2020 and 10.54499/UIDP/04516/2020) with the financial support of FCT.IP (2021.05646.BD) and the Recovery and Resilience Plan under the application nº 761 submitted to the measure Polos de Inovação Digital (DIH) under the terms of AAC nº. 03/C16 i03/2022. Finally, we would like to acknowledge Audrey Aldridge, Carolina Jorge, Diego Andres Blanco-Mora, Sofia Ferreira, Mónica Rosa, and Sidonio Fernandes for assisting with the patient's preparation and data acquisition at the hospital.

Ethics approval and consent to participate

This study was performed in accordance with the Declaration of Helsinki. This human study was approved by Scientific and Ethic Committees of the Central Hospital of Funchal, Portugal - approval: 21/2019. The study's clinical trial registration number is NCT04376138 registered with https://clinicaltrials.gov/study/NCT04376138. Participant registration took place from Aug-2019 to Dec-2023. All adult participants provided written informed consent to participate in this study.

Consent for publication

All participants provided written informed consent for the publication of anonymized data included in this manuscript.

Availability of data and materials

All participants were anonymized by assigning a unique study code. De-identified participant data, the corresponding data dictionary, and statistical code used for analyses are available upon reasonable request from the corresponding author.

Competing interests

We declare that the authors have no competing interests as defined by BMC, or other interests that might be perceived to influence the results and/or discussion reported in this paper.

Funding

This work is supported financially by FCT through the LARSyS - FCT Project (DOI: 10.54499/LA/P/0083/2020, 10.54499/UIDP/50009/2020, and 10.54499/UIDB/50009/2020), the NeurAugVR (PTDC/CCI-COM/31485/2017), the NOISyS project (DOI: 10.54499/2022.02283.PTDC), the FCT grant: 10.54499/2021.05646.BD, the NOVA LINCS (DOI: 10.54499/UIDB/04516/2020 and 10.54499/UIDP/04516/2020) with the financial support of FCT.IP (2021.05646.BD) and the Recovery and Resilience Plan under the application nº 761 submitted to the measure Polos de Inovação Digital (DIH) under the terms of AAC nº. 03/C16 i03/2022.

Authors' contributions

MV contributed to data curation, formal analysis, investigation, visualization, and drafting of the manuscript. DB and JC-F contributed to data curation, investigation, validation, and critical manuscript review and editing. SBB contributed to conceptualization, funding acquisition, project administration, provision of resources, investigation, and critical manuscript review and editing. PF contributed to conceptualization, funding acquisition, supervision, validation, provision of resources, investigation, and critical manuscript review and editing. AV contributed to conceptualization, investigation, methodology development, software implementation, supervision, validation, provision of resources, and critical manuscript review and editing. All authors read and approved the final manuscript.

References

1. Feigin VL, Brainin M, Norrving B, Martins S, Sacco RL, Hacke W, Fisher M, Pandian J, and Lindsay P. World Stroke Organization (WSO): Global Stroke Fact Sheet 2022. International Journal of Stroke 2022; 17. PMID: 34986727:18–29. DOI: 10.1177/17474930211065917
2. Cioni G, Sgandurra G, Muzzini S, Paolicelli PB, and Ferrari A. Forms of Hemiplegia. *The Spastic Forms of Cerebral Palsy: A Guide to the Assessment of Adaptive Functions*. Milano: Springer Milan, 2010 :331–56. DOI: 10.1007/978-88-470-1478-7_16
3. Bonita R and Beaglehole R. Recovery of motor function after stroke. Stroke 1988; 19:1497–500. DOI: 10.1161/01.STR.19.12.1497

REFERENCES

4. Dobkin BH. Strategies for stroke rehabilitation. The Lancet Neurology 2004; 3:528–36. DOI: https://doi.org/10.1016/S1474-4422(04)00851-8
5. Cuccurullo SJ. Physical medicine and rehabilitation board review. Springer Publishing Company, 2019
6. Laver KE, Lange B, George S, Deutsch JE, Saposnik G, Chapman M, and Crotty M. Virtual reality for stroke rehabilitation. Cochrane database of systematic reviews 2025. Available from: https://doi.org//10.1002/14651858.CD008349.pub5
7. Cervera MA, Soekadar SR, Ushiba J, Millán JDR, Liu M, Birbaumer N, and Garipelli G. Brain-computer interfaces for post-stroke motor rehabilitation: a meta-analysis. Annals of Clinical and Translational Neurology. 2018 May; 5:651–63. DOI: 10.1002/acn3.544. Available from: https://onlinelibrary.wiley.com/doi/10.1002/acn3.544 [Accessed on: 2025 Oct 29]
8. Yang W, Zhang X, Li Z, Zhang Q, Xue C, and Huai Y. The Effect of Brain–Computer Interface Training on Rehabilitation of Upper Limb Dysfunction After Stroke: A Meta-Analysis of Randomized Controlled Trials. Frontiers in Neuroscience. 2022 Feb 7; 15:766879. DOI: 10.3389/fnins.2021.766879. Available from: https://www.frontiersin.org/articles/10.3389/fnins.2021.766879/full [Accessed on: 2025 Oct 29]
9. Tonin A, Semprini M, Kiper P, and Mantini D. Brain-Computer Interfaces for Stroke Motor Rehabilitation. Bioengineering. 2025 Jul 30; 12:820. DOI: 10.3390/bioengineering12080820. Available from: https://www.mdpi.com/2306-5354/12/8/820 [Accessed on: 2025 Oct 29]
10. Leeb R and Pérez-Marcos D. Brain-computer interfaces and virtual reality for neurorehabilitation. Handbook of clinical neurology 2020; 168:183–97
11. Pichiorri F, Morone G, Petti M, Toppi J, Pisotta I, Molinari M, Paolucci S, Inghilleri M, Astolfi L, Cincotti F, et al. Brain–computer interface boosts motor imagery practice during stroke recovery. Annals of neurology 2015; 77:851–65
12. Li D, Li R, Song Y, Qin W, Sun G, Liu Y, Bao Y, Liu L, and Jin L. Effects of brain-computer interface based training on post-stroke upper-limb rehabilitation: a meta-analysis. Journal of NeuroEngineering and Rehabilitation. 2025 Mar 3; 22:44. DOI: 10.1186/s12984-025-01588-x. Available from: https://jneuroengrehab.biomedcentral.com/articles/10.1186/s12984-025-01588-x [Accessed on: 2025 Oct 29]
13. Alashram AR, Padua E, and Annino G. Effects of Brain-Computer Interface Controlled Functional Electrical Stimulation on Motor Recovery in Stroke Survivors: a Systematic Review. Current Physical Medicine and Rehabilitation Reports. 2022 Sep 14; 10:299–310. DOI: 10.1007/s40141-022-00369-0. Available from: https://link.springer.com/10.1007/s40141-022-00369-0 [Accessed on: 2025 Oct 29]

REFERENCES

14. Liu J, Li Y, Zhao D, Zhong L, Wang Y, Hao M, and Ma J. Efficacy and safety of brain–computer interface for stroke rehabilitation: an overview of systematic review. Frontiers in Human Neuroscience. 2025 Mar 6; 19:1525293. DOI: 10.3389/fnhum.2025.1525293. Available from: https://www.frontiersin.org/articles/10.3389/fnhum.2025.1525293/full [Accessed on: 2025 Oct 29]

15. Ren C, Li X, Gao Q, Pan M, Wang J, Yang F, Duan Z, Guo P, and Zhang Y. The effect of brain-computer interface controlled functional electrical stimulation training on rehabilitation of upper limb after stroke: a systematic review and meta-analysis. Frontiers in Human Neuroscience. 2024 Sep 26; 18:1438095. DOI: 10.3389/fnhum.2024.1438095. Available from: https://www.frontiersin.org/articles/10.3389/fnhum.2024.1438095/full [Accessed on: 2025 Oct 29]

16. Zhang M, Zhu F, Jia F, Wu Y, Wang B, Gao L, Chu F, and Tang W. Efficacy of brain-computer interfaces on upper extremity motor function rehabilitation after stroke: A systematic review and meta-analysis. NeuroRehabilitation. 2024 Mar 11; 54:199–212. DOI: 10.3233/NRE-230215. Available from: https://journals.sagepub.com/doi/full/10.3233/NRE-230215 [Accessed on: 2025 Oct 29]

17. Ma Yn, Karako K, Song P, Hu X, and Xia Y. Integrative neurorehabilitation using brain-computer interface: From motor function to mental health after stroke. BioScience Trends. 2025 Jun 30; 19:243–51. DOI: 10.5582/bst.2025.01109. Available from: https://www.jstage.jst.go.jp/article/bst/19/3/19_2025.01109/_article [Accessed on: 2025 Oct 29]

18. López-Larraz E, Sarasola-Sanz A, Irastorza-Landa N, Birbaumer N, and Ramos-Murguialday A. Brain-machine interfaces for rehabilitation in stroke: A review. NeuroRehabilitation. 2018 Jul 24; 43. Ed. by Harvey RL:77–97. DOI: 10.3233/NRE-172394. Available from: https://journals.sagepub.com/doi/full/10.3233/NRE-172394 [Accessed on: 2025 Oct 29]

19. Neuper C, Scherer R, Wriessnegger S, and Pfurtscheller G. Motor imagery and action observation: Modulation of sensorimotor brain rhythms during mental control of a brain–computer interface. Clinical Neurophysiology 2009; 120:239–47. DOI: https://doi.org/10.1016/j.clinph.2008.11.015

20. Pfurtscheller G and Aranibar A. Event-related cortical desynchronization detected by power measurements of scalp EEG. Electroencephalography and Clinical Neurophysiology 1977; 42:817–26. DOI: https://doi.org/10.1016/0013-4694(77)90235-8

21. Ray AM, Figueiredo TDC, López-Larraz E, Birbaumer N, and Ramos-Murguialday A. Brain oscillatory activity as a biomarker of motor recovery in chronic stroke. Human Brain Mapping. 2020 Apr; 41:1296–308. DOI: 10.1002/hbm.24876. Available from: https://onlinelibrary.wiley.com/doi/10.1002/hbm.24876 [Accessed on: 2025 Oct 23]

REFERENCES

22. Remsik AB, Gjini K, Williams L, Van Kan PLE, Gloe S, Bjorklund E, Rivera CA, Romero S, Young BM, Nair VA, Caldera KE, Williams JC, and Prabhakaran V. Ipsilesional Mu Rhythm Desynchronization Correlates With Improvements in Affected Hand Grip Strength and Functional Connectivity in Sensorimotor Cortices Following BCI-FES Intervention for Upper Extremity in Stroke Survivors. Frontiers in Human Neuroscience. 2021 Oct 28; 15:725645. DOI: 10.3389/fnhum.2021.725645. Available from: https://www.frontiersin.org/articles/10.3389/fnhum.2021.725645/full [Accessed on: 2025 Oct 23]

23. Kancheva I, Van Der Salm SMA, Ramsey NF, and Vansteensel MJ. Association between lesion location and sensorimotor rhythms in stroke – a systematic review with narrative synthesis. Neurological Sciences. 2023 Dec; 44:4263–89. DOI: 10.1007/s10072-023-06982-8. Available from: https://link.springer.com/10.1007/s10072-023-06982-8 [Accessed on: 2025 Oct 23]

24. Rustamov N, Souders L, Sheehan L, Carter A, and Leuthardt EC. IpsiHand Brain-Computer Interface Therapy Induces Broad Upper Extremity Motor Recovery in Chronic Stroke. 2023 Aug 28. DOI: 10.1101/2023.08.26.23294320. Available from: http://medrxiv.org/lookup/doi/10.1101/2023.08.26.23294320 [Accessed on: 2025 Oct 23]

25. Gangadharan SK, Ramakrishnan S, Paek A, Ravindran A, Prasad VA, and Vidal JLC. Characterization of Event Related Desynchronization in Chronic Stroke Using Motor Imagery Based Brain Computer Interface for Upper Limb Rehabilitation. Annals of Indian Academy of Neurology. 2024 Jun 5. DOI: 10.4103/aian.aian_1056_23. Available from: https://journals.lww.com/10.4103/aian.aian_1056_23 [Accessed on: 2025 Oct 23]

26. Vourvopoulos A, Blanco-Mora D, Aldridge A, Jorge C, Fernandes JC, Figueiredo P, and Badia SBI. Influence of VR-based Brain-Computer Interfaces Training in Brain Activity and Clinical Outcome in Chronic Stroke: A Longitudinal Study of Single Cases. 2022 Oct 27. DOI: 10.21203/rs.3.rs-2193322/v1. Available from: https://www.researchsquare.com/article/rs-2193322/v1 [Accessed on: 2025 Oct 23]

27. Sebastian-Romagosa M, Ortner R, Udina-Bonet E, Dinares-Ferran J, Mayr K, Cao F, and Guger C. Laterality Coefficient: An EEG parameter related with the functional improvement in stroke patients. *2019 IEEE EMBS International Conference on Biomedical & Health Informatics (BHI)*. 2019 IEEE EMBS International Conference on Biomedical & Health Informatics (BHI). Chicago, IL, USA: IEEE, 2019 May :1–4. DOI: 10.1109/BHI.2019.8834472. Available from: https://ieeexplore.ieee.org/document/8834472/ [Accessed on: 2025 Oct 23]

28. Sebastián-Romagosa M, Udina E, Ortner R, Dinarès-Ferran J, Cho W, Murovec N, Matencio-Peralba C, Sieghartsleitner S, Allison BZ, and Guger C. EEG biomarkers

related with the functional state of stroke patients. Frontiers in neuroscience 2020; 14:582

29. Mansour S, Giles J, Ang KK, Nair KPS, Phua KS, and Arvaneh M. Exploring the ability of stroke survivors in using the contralesional hemisphere to control a brain–computer interface. Scientific Reports. 2022 Sep 28; 12:16223. DOI: 10.1038/s41598-022-20345-x. Available from: https://www.nature.com/articles/s41598-022-20345-x [Accessed on: 2025 Oct 23]
30. Liu XY, Wang WL, Liu M, Chen MY, Pereira T, Doda DY, Ke YF, Wang SY, Wen D, Tong XG, et al. Recent applications of EEG-based brain-computer-interface in the medical field. Military Medical Research 2025; 12:14
31. Chen S, Chen M, Wang X, Liu X, Liu B, and Ming D. Brain–computer interfaces in 2023–2024. Brain-X 2025; 3:e70024
32. Heruti RJ, Lusky A, Dankner R, Ring H, Dolgopiat M, Barell V, Levenkrohn S, and Adunsky A. Rehabilitation outcome of elderly patients after a first stroke: Effect of cognitive status at admission on the functional outcome. Archives of Physical Medicine and Rehabilitation 2002; 83:742–9. DOI: https://doi.org/10.1053/apmr.2002.32739
33. Bagg S, Pombo AP, and Hopman W. Effect of Age on Functional Outcomes After Stroke Rehabilitation. Stroke 2002; 33:179–85. DOI: 10.1161/hs0102.101224
34. Ramos-Murguialday A, Broetz D, Rea M, Läer L, Yilmaz Ö, Brasil FL, Liberati G, Curado MR, Garcia-Cossio E, Vyziotis A, Cho W, Agostini M, Soares E, Soekadar S, Caria A, Cohen LG, and Birbaumer N. Brain–machine interface in chronic stroke rehabilitation: A controlled study. Annals of Neurology 2013; 74:100–8. DOI: https://doi.org/10.1002/ana.23879
35. Pollok B, Latz D, Krause V, Butz M, and Schnitzler A. Changes of motor-cortical oscillations associated with motor learning. Neuroscience 2014; 275:47–53
36. Lotte F, Larrue F, and Mühl C. Flaws in current human training protocols for spontaneous Brain-Computer Interfaces: lessons learned from instructional design. Frontiers in Human Neuroscience 2013; 7
37. Jeunet C, Jahanpour E, and Lotte F. Why standard brain-computer interface (BCI) training protocols should be changed: an experimental study. Journal of neural engineering 2016; 13:036024
38. Perdikis S and Millan JdR. Brain-machine interfaces: a tale of two learners. IEEE Systems, Man, and Cybernetics Magazine 2020; 6:12–9
39. Vavoulis A, Figueiredo P, and Vourvopoulos A. A Review of Online Classification Performance in Motor Imagery-Based Brain–Computer Interfaces for Stroke Neurorehabilitation. Signals 2023; 4:73–86. DOI: 10.3390/signals4010004

REFERENCES

40. Vourvopoulos A and Badia SBI. Usability and Cost-effectiveness in Brain-Computer Interaction: Is it User Throughput or Technology Related? *Proceedings of the 7th Augmented Human International Conference 2016*. AH '16: Augmented Human International Conference 2016. Geneva Switzerland: ACM, 2016 Feb 25:1–8. DOI: 10.1145/2875194.2875244. Available from: https://dl.acm.org/doi/10.1145/2875194.2875244 [Accessed on: 2025 Oct 29]

41. Vourvopoulos A, Ferreira A, and Badia SBI. NeuRow: An Immersive VR Environment for Motor-Imagery Training with the Use of Brain-Computer Interfaces and Vibrotactile Feedback: *Proceedings of the 3rd International Conference on Physiological Computing Systems*. 3rd International Conference on Physiological Computing Systems. Lisbon, Portugal: SCITEPRESS - Science and Technology Publications, 2016 :43–53. DOI: 10.5220/0005939400430053. Available from: http://www.scitepress.org/DigitalLibrary/Link.aspx?doi=10.5220/0005939400430053 [Accessed on: 2025 Oct 29]

42. Vourvopoulos A and Bermúdez I Badia S. Motor priming in virtual reality can augment motor-imagery training efficacy in restorative brain-computer interaction: a within-subject analysis. Journal of NeuroEngineering and Rehabilitation. 2016 Dec; 13:69. DOI: 10.1186/s12984-016-0173-2. Available from: http://jneuroengrehab.biomedcentral.com/articles/10.1186/s12984-016-0173-2 [Accessed on: 2025 Oct 29]

43. Vourvopoulos A, Marin-Pardo O, Neureither M, Saldana D, Jahng E, and Liew SL. Multimodal Head-Mounted Virtual-Reality Brain-Computer Interface for Stroke Rehabilitation: A Clinical Case Study with REINVENT. *Virtual, Augmented and Mixed Reality. Multimodal Interaction*. Ed. by Chen JY and Fragomeni G. Vol. 11574. Series Title: Lecture Notes in Computer Science. Cham: Springer International Publishing, 2019 :165–79. DOI: 10.1007/978-3-030-21607-8_13. Available from: https://link.springer.com/10.1007/978-3-030-21607-8_13 [Accessed on: 2025 Oct 29]

44. Vourvopoulos A, Pardo OM, Lefebvre S, Neureither M, Saldana D, Jahng E, and Liew SL. Effects of a Brain-Computer Interface With Virtual Reality (VR) Neurofeedback: A Pilot Study in Chronic Stroke Patients. Frontiers in Human Neuroscience. 2019 Jun 19; 13:210. DOI: 10.3389/fnhum.2019.00210. Available from: https://www.frontiersin.org/article/10.3389/fnhum.2019.00210/full [Accessed on: 2025 Oct 29]

45. Lupu RG, Irimia DC, Ungureanu F, Poboroniuc MS, and Moldoveanu A. BCI and FES Based Therapy for Stroke Rehabilitation Using VR Facilities. Wireless Communications and Mobile Computing. 2018 Jan; 2018. Ed. by Konstantinidis EI:4798359. DOI: 10.1155/2018/4798359. Available from: https://onlinelibrary.wiley.com/doi/10.1155/2018/4798359 [Accessed on: 2025 Oct 29]

REFERENCES

46. Brain EBS. Intra-and Inter-subject Variability in. Inter-and Intra-subject Variability in Brain Imaging and Decoding 2022 :8722
47. Yesavage JA, Brink TL, Rose TL, Lum O, Huang V, Adey M, and Leirer VO. Development and validation of a geriatric depression screening scale: a preliminary report. Journal of psychiatric research 1982; 17:37–49
48. Blanco-Mora D, Aldridge A, Jorge C, Vourvopoulos A, Figueiredo P, and Bermúdez I Badia S. Impact of age, VR, immersion, and spatial resolution on classifier performance for a MI-based BCI. Brain-Computer Interfaces 2022; 9:169–78
49. Vourvopoulos A, Blanco-Mora DA, Aldridge A, Jorge C, Figueiredo P, and Badia SB i. Enhancing motor-imagery brain-computer interface training with embodied virtual reality: a pilot study with older adults. *2022 IEEE International Conference on Metrology for Extended Reality, Artificial Intelligence and Neural Engineering (MetroXRAINE)*. IEEE. 2022 :157–62
50. Batista D, Caetano G, Fleury M, Figueiredo P, and Vourvopoulos A. Effect of head-mounted virtual reality and vibrotactile feedback in ERD during motor imagery Brain–computer interface training. Brain-Computer Interfaces 2024; 11:11–20
51. Gladstone DJ, Danells CJ, and Black SE. The Fugl-Meyer Assessment of Motor Recovery after Stroke: A Critical Review of Its Measurement Properties. Neurorehabilitation and Neural Repair 2002; 16. PMID: 12234086:232–40. DOI: 10.1177/154596802401105171
52. Page SJ, Fulk GD, and Boyne P. Clinically Important Differences for the Upper-Extremity Fugl-Meyer Scale in People With Minimal to Moderate Impairment Due to Chronic Stroke. Physical Therapy 2012 Jun; 92:791–8. DOI: 10.2522/ptj.20110009
53. Nasreddine ZS, Phillips NA, Bédirian V, Charbonneau S, Whitehead V, Collin I, Cummings JL, and Chertkow H. The Montreal Cognitive Assessment, MoCA: A Brief Screening Tool For Mild Cognitive Impairment. Journal of the American Geriatrics Society 2005; 53:695–9. DOI: https://doi.org/10.1111/j.1532-5415.2005.53221.x
54. Malouin F, Richards CL, Jackson PL, Lafleur MF, Durand A, and Doyon J. The Kinesthetic and Visual Imagery Questionnaire (KVIQ) for assessing motor imagery in persons with physical disabilities: a reliability and construct validity study. Journal of neurologic physical therapy 2007; 31:20–9
55. Vourvopoulos A, Ferreira A, and Badia SB i. NeuRow: an immersive VR environment for motor-imagery training with the use of brain-computer interfaces and vibrotactile feedback. *International Conference on Physiological Computing Systems*. Vol. 2. SciTePress. 2016 :43–53. DOI: 10.5220/0005939400430053
56. Lotte F, Bougrain L, Cichocki A, Clerc M, Congedo M, Rakotomamonjy A, and Yger F. A review of classification algorithms for EEG-based brain–computer interfaces: a 10 year update. Journal of Neural Engineering 2018 Apr; 15:031005. DOI: 10.1088/1741-2552/aab2f2

57. Vourvopoulos A, Fleury M, Blanco-Mora DA, Fernandes JC, Figueiredo P1, and Bermúdez i Badia S. Brain imaging and clinical outcome of embodied VR-BCI training in chronic stroke patients: a longitudinal pilot study. Brain-Computer Interfaces 2024; 11:193–209

58. Cauraugh JH and Summers JJ. Neural plasticity and bilateral movements: A rehabilitation approach for chronic stroke. Progress in Neurobiology 2005; 75:309–20

59. Palmer JA, Wheaton LA, Gray WA, Saltão da Silva MA, Wolf SL, and Borich MR. Role of interhemispheric cortical interactions in poststroke motor function. Neurorehabilitation and Neural Repair 2019; 33:762–74

60. Summers JJ, Kagerer FA, Garry MI, Hiraga CY, Loftus A, and Cauraugh JH. Bilateral and unilateral movement training on upper limb function in chronic stroke patients: A TMS study. Journal of the Neurological Sciences 2007; 252:76–82

61. Rizzolatti G and Craighero L. The mirror-neuron system. Annual Review of Neuroscience 2004; 27:169–92

62. Garrison KA, Winstein CJ, and Aziz-Zadeh L. The mirror neuron system: A neural substrate for methods in stroke rehabilitation. Neurorehabilitation and Neural Repair 2010; 24:404–12

63. Ertelt D, Small S, Solodkin A, Dettmers C, McNamara A, Binkofski F, and Buccino G. Action observation has a positive impact on rehabilitation of motor deficits after stroke. NeuroImage 2007; 36:T164–T173

64. Neuper C and Pfurtscheller G. Event-related dynamics of cortical rhythms: frequency-specific features and functional correlates. International journal of psychophysiology 2001; 43:41–58

65. Pineda JA. Sensorimotor cortex as a critical component of an'extended'mirror neuron system: Does it solve the development, correspondence, and control problems in mirroring? Behavioral and Brain Functions 2008; 4:47

66. Nunes JD, Vourvopoulos A, Blanco-Mora DA, Jorge C, Fernandes JC, Bermudez i Badia S, and Figueiredo P. Brain activation by a VR-based motor imagery and observation task: An fMRI study. Plos one 2023; 18:e0291528

67. Pfurtscheller G, Neuper C, Brunner C, and Da Silva FL. Beta rebound after different types of motor imagery in man. Neuroscience letters 2005; 378:156–9

68. Ray A, Figueiredo T, López-Larraz E, Birbaumer N, Ramos-Murguialday A, López-Larraz E, and Ramos-Murguialday A. Brain oscillatory activity as a biomarker of motor recovery in chronic stroke. English. Human Brain Mapping 2020 Apr; 41. Publisher Copyright: © 2019 The Authors. Human Brain Mapping published by Wiley Periodicals, Inc.:1296–308. DOI: 10.1002/hbm.24876

REFERENCES

69. Biasiucci A, Leeb R, Iturrate I, Perdikis S, Al-Khodairy A, Corbet T, Schnider A, Schmidlin T, Zhang H, Bassolino M, et al. Brain-actuated functional electrical stimulation elicits lasting arm motor recovery after stroke. Nature communications 2018; 9:2421
70. Delorme A and Makeig S. EEGLAB: an open source toolbox for analysis of single-trial EEG dynamics including independent component analysis. Journal of Neuroscience Methods 2004; 134:9–21. DOI: https://doi.org/10.1016/j.jneumeth.2003.10.009
71. Kothe C and Jung T. Artifact removal techniques with signal reconstruction. US Patent App. 14/895,440. 2016
72. Plechawska-Wojcik M, Kaczorowska M, and Zapala D. The artifact subspace reconstruction (ASR) for EEG signal correction. A comparative study. *Information systems architecture and technology: proceedings of 39th international conference on information systems architecture and technology–ISAT 2018: part II*. Springer. 2019 :125–35
73. Makeig S, Bell A, Jung TP, and Sejnowski TJ. Independent Component Analysis of Electroencephalographic Data. *Advances in Neural Information Processing Systems*. Ed. by Touretzky D, Mozer M, and Hasselmo M. Vol. 8. MIT Press, 1995
74. Pion-Tonachini L, Kreutz-Delgado K, and Makeig S. ICLabel: An automated electroencephalographic independent component classifier, dataset, and website. NeuroImage 2019; 198:181–97. DOI: https://doi.org/10.1016/j.neuroimage.2019.05.026
75. Pfurtscheller G and Lopes da Silva F. Event-related EEG/MEG synchronization and desynchronization: basic principles. Clinical Neurophysiology 1999; 110:1842–57. DOI: https://doi.org/10.1016/S1388-2457(99)00141-8
76. Medvedeva A, Syrov N, Yakovlev L, Alieva YA, Petrova D, Ivanova G, Lebedev M, and Kaplan AY. Event-related desynchronization of eeg sensorimotor rhythms in hemiparesis post-stroke patients. Journal of Evolutionary Biochemistry and Physiology 2024; 60:2058–71
77. Doyle LM, Yarrow K, and Brown P. Lateralization of event-related beta desynchronization in the EEG during pre-cued reaction time tasks. Clinical Neurophysiology 2005; 116:1879–88. DOI: https://doi.org/10.1016/j.clinph.2005.03.017
78. Kaiser V, Daly I, Pichiorri F, Mattia D, Müller-Putz GR, and Neuper C. Relationship between electrical brain responses to motor imagery and motor impairment in stroke. Stroke 2012; 43:2735–40
79. Afonso M, Sánchez-Cuesta F, González-Zamorano Y, Romero Muñoz JP, and Vourvopoulos A. Investigating the synergistic neuromodulation effect of bilateral rTMS and VR brain-computer interfaces training in chronic stroke patients. Journal of Neural Engineering 2024 Oct; 21. DOI: 10.1088/1741-2552/ad8836

REFERENCES

80. Shetty V, Morrell CH, and Najjar SS. Modeling a cross-sectional response variable with longitudinal predictors: an example of pulse pressure and pulse wave velocity. Journal of applied statistics 2009; 36:611–9

81. Langhorne P, Bernhardt J, and Kwakkel G. Stroke rehabilitation. The Lancet 2011; 377:1693–702

82. Stępień M, Conradi J, Waterstraat G, Hohlefeld FU, Curio G, and Nikulin VV. Event-related desynchronization of sensorimotor EEG rhythms in hemiparetic patients with acute stroke. Neuroscience letters 2011; 488:17–21

83. Takeuchi N and Izumi SI. Maladaptive plasticity for motor recovery after stroke: mechanisms and approaches. Neural plasticity 2012; 2012:359728